Characterization of Deep Levels Induced By MeV He^+ Ions In Si Photodiode

By

Sasmita Dehury

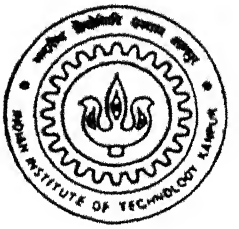

Material Science Program,

INDIAN INSTITUTE OF TECHNOLOGY, KANPUR

DECEMBER, 1998

Characterization of Deep levels Induced By MeV He^+ Ions In Si Photodiode

A thesis submitted in
Partial fulfillment of the requirements
for the degree of
Master of Technology

by
Sasmita Dehury

Material Science Program,
Indian Institute of Technology, Kanpur.
December 1998

CERTIFICATE

It is certified that the work contained in the thesis entitled "**Characterization Of Deep Levels Induced By MeV He^+ Ions In Si Photodiode**" by ***Sasmita Dehury*** has been carried out under our supervision and has not been submitted elsewhere for a degree.

Dr.Y.N.Mohapatra.
Material Science Programme
I.I.T Kanpur.

Dr V N Kulkarni.
Department of Physics
I.I.T.Kanpur.

Dedicated

to

My Parents

ACKNOWLEDGEMENT

I am deeply indebted to my thesis advisers Dr.Y.N.Mohapatra and Dr.V.N.Kulkarni for their interest in successful completion of this thesis. I take this opportunity to express my gratitude to Dr.Y.N.Mohapatra for bringing me to this exciting branch of physics which was able to instill a deep sense of interest in me. I am also thankful to Dr.V.N.Kulkarni for his valuable guidance. They helped me with advice and guidance when I most needed it. Working with them has been a rewarding experience.

I express my gratitude to all of my teachers till now.

I must thank the staffs of ACMS workshop for their co-operation during my experiments. I am also grateful to the members of nuclear physics lab for their invaluable help in my work I would like to thank many of my friends and persons who have made my stay here an immensely educative experience.

I am specially thankful to Sangeeta for being co-operative and helpful through out my work. Without her help, it would not have been possible to do all the work that has been done. My best wishes are always there for her. I am also grateful to Giri da and Anirban for their co-operation and help at various stages of my work.

I wish to thank Sarika, Tripti , Jayashree and Sanghamitra who often shared their time and company when I needed it most . They have made my stay at IIT,Kanpur memorable and cherisable .

Finally , I acknowledge my parents , my sisters , brother - in -laws and my brother for their love and care. I will always remain grateful to GOD for his blessings on me.

SASMITA DEHURY

CONTENTS

LIST OF FIGURES

LIST OF TABLES

ABSTRACT

The study of damage and electrically active traps induced by MeV He^+ ions in semiconductors is important from both fundamental and application point of view. In this work we choose to study in terms of electrically active traps induced by MeV alpha particles in the active layer of a commercially available Si photodiode. The sample is irradiated with 1.26 MeV He^+ ions with a dose of $1x10^{10}$ cm^{-2} at room temperature creating damage upto 4 μm deep in the sample as obtained from the TRIM simulation. The spectroscopic methods such as deep level transient spectroscopy (DLTS), thermally stimulated capacitance spectroscopy (TSCAP) and time analyzed transient spectroscopy (TATS) in the temperature range of 90 K - 300 K were used after irradiations in the sample. The existing spectrometer was augmented to be able to carry out optical filling of traps for the purpose of characterization.

As the zero bias depletion width is very wide due to the intrinsic character of the active layer of a pin photodiode, conventional DLTS and related pulsing techniques are not suitable for detecting traps Instead optical pulsing to fill the traps was found to be convenient. No active deep traps were found prior to irradiation in the active layer with concentration more than 10^9 cm^{-3} . After irradiation three minority carrier peaks and one majority carrier peak was observed in DLTS with concentrations approximately of the same order as background doping. Time analyzed transient spectroscopy based on analysis of isothermal transient also show these peaks. From Arrhenius analysis the activation energies of the traps are found to be 0.23 eV , 0.30 eV and 0.5 eV The majority carrier trap has an activation energy of 0.57 eV The 0.23 eV is the dominant peak. Lineshape analysis of 0.23 eV peak shows that it does not correspond to a discrete level in the gap and is probably distributed in energy due to disorder TATS lineshape analysis of the 0 23 peak shows that it is more likely to be composed of two closely lying energy levels. The majority carrier peak at 0.57 eV is exponential in character, though distorted by the presence of minority carrier peak preceding it. The majority carrier trap is attributed to a hole emitting center often found in irradiation induced damage in p- type material. The 0.23 eV is due to the first ionization of divacancy emitting an electron to the conduction band. However corresponding second ionization electron trap at E_C -0.42 eV is not observed. The advantages and disadvantages of using photodiodes for MeV particle irradiation studies are discussed.

CHAPTER 1

INTRODUCTION

1.1 INTRODUCTION

Imperfection in solids perturb the periodicity of the crystal They are important because they control the electrical , optical , thermal and mechanical properties of solids. In solid state devices such as the bipolar transistors , the MOS field - effect transistors , the light emitting diodes and the junction lasers , and the tunnel diodes etc. , impurity and imperfection centers control vital electrical and optical characteristics While in some cases such as lasers and LEDs they have to be avoided in others they are deliberately introduced .

In semiconductors , some of the impurities are intentionally introduced to serve as dopant atoms (shallow - level impurities) , recombination centers (deep - level impurities) to reduce the device lifetime , or deep - level impurities to increase the substrate resistivity. Many impurities are unintentionally incorporated during crystal growth and device processing The impurities may be foreign impurities (e.g., metals) , crystallographic point defects (e.g., vacancies and interstitial) , or structural defects (e.g., stacking faults and dislocations) .

Thus the electrical , optical and optoelectronic properties of a semiconductor are therefore significantly controlled by the presence of impurities and defects . Hence there has been over the years an increasing importance of characterizing these defects and impurities , and elucidating their role in optoelectronic properties relevant to applications .

In this work we aim to study the electrical characterization of defects in semiconductors induced by high energy radiation . This is one of the areas of research for both fundamental reasons and applications [1]

1.2. TECHNOLOGICAL ADVANTAGES OF HIGH ENERGY ION IMPLANTATION

Low energy KeV range implants are now industrially standardized routine processing tool .High energy ion implantation is an important technology especially in the area of semiconductor device fabrication Its main application has been in highly controlled doping of semiconductors It possesses some clear advantages over , and thereby compliments , other processing methods The technology benefits greatly from studies on the damage caused in materials by ion implantation . On the other hand a satisfactory understanding of damage has shown that it need not always be the undesirable feature of ion implantation and may in fact be used to advantage in device fabrication [2]

- The reduction in carrier mobility resulting from damage in partially annealed implants has made it possible to fabricate high - value resistors in silicon Even by annealing the damage to appropriate degree ,resistors with a zero temperature coefficient of resistance have been fabricated .
- Damage may be used as a 'life-time-killer' . Proton implantation damage in compound semiconductors contains optical absorption centers This is used for optically isolating light-emitting diode lasers and for the fabrication of wave guides in optical integrated circuits .
- Carrier trapping in the region of damage created by proton bombardment may be used to provide electrical isolation of individual integrated circuit elements . These introduce unwanted capacitance which limits the operational speed of the circuit and are voltage and temperature sensitive.
- Ion implantation damage studies are of widespread importance in scientific and industrial research . Solid state electronics systems operating in earth satellites are subject to high energetic particles . The resulting damage causes lowered rectification ratio of diodes , lowered gain of transistors and lowered power output of solar cells and failure of devices .

These advantages have specifically become important with the emergence of MeV ion implantation over last ten years . However success of MeV ion implantation is crucially dependent on a through understanding of damage associated with the process More specifically the characterization of electrically active trap levels induced by damage has become a key issue to the success of this technology .

This work is devoted to characterization of deep levels introduced into the active layer of a photodiode using MeV alpha particles . Before stating our motivation and exact nature of the problem we first give below a brief review of defects induced in silicon by MeV ions with focus on results of characterization techniques used in this work .

1.3.A REVIEW ON DEFECTS INDUCED BY ENERGETIC IONS

1.3.1. Background

In a semiconductor imperfections can be introduced by photoexcitation , X-rays , γ-rays , electrons and other particle irradiation ,and by electrical injection at pn junctions . Defect creation in semiconductor due to radiation damage has been extensively studied for the past twenty - five years . This review presents a cursory glance at the previous work done on this field .

As already mentioned, implantation of energetic ions into crystalline semiconductor gives rise to atomic displacement and structural defects . The generation of stable defects depends on several parameters, e.g., ion energy, ion mass , sample temperature , ion dose and dose rate . For light particles and low fluences only point defects are produced while for high fluences of heavy particles one encounters the other extremes of amorphous layers . These are the two extremes regimes of MeV implants that have been studied in recent years though with different methods .

Incident particles of sufficient energy can displace silicon atoms from lattice positions , thus creating interstitial - vacancy complexes .These defects are unstable at room temperature and thus observed as defect complexes [3] . The hierarchy of

stable defects generated from primary defects such as frenkle pairs , vacancies and interstitial have been most thoroughly studied for electron irradiation . These intrinsic pair among themselves or with commonly found impurities such as carbon , oxygen or with other dopants . Some of the well known interstitial complexes are C_s -C_i ,C_i -O_i ,B_i-B_s ,while vacancy complexes includes divacancy V_2 , V- O ,V -P .

The divacancy (V_2) , A center (oxygen - vacancy complex) and E center (donor - vacancy complex) are the well identified defect complexes commonly observed in various studies in n - silicon . A summary of energy and capture cross-section of reported defect levels in as - implanted n - Si is presented in table 1[4].

These point defects have been studied in great detail by techniques such as electron paramagnetic resonance (EPR)[5] , infrared detection technique (IR) [6] , and deep level transient spectroscopy (DLTS) [7,8,9,10] Although a lot of work have been done in the low damage regime , specially with light particles such as electrons , neutrons and protons but it is only recently that there have been studies on similar point defects generated by **heavy ions** in MeV range by keeping the fluences of the ion very small ($<10^9$ cm^{-2}) [11]. In this regime of defects , identification of electrical signature of the defects have played a central role in determining their nature and properties .

Recently , work has also been carried out in intermediate regime of damage .This regime of damage could not be detected by any conventional probing techniques but plays an important role in many phenomena of current interest such as defect clustering , transient enhanced diffusion , modification of properties of buried layers as in rare - earth doping , etc. In a recent study , Benton et al . [11] have attempted to trace the evolution of damage induced by MeV Si ions in Si with dose and annealing in an effort to provide what they term as the **"missing link"** between point defects and **extended defect regimes .**

The assignment of defect identification has been less straight forward in case of p - type silicon . This may be attributed to a general lack of consensus in the literature

regarding the identity of similar defect levels observed in electron irradiated p -Si . Divacancy and interstitial - carbon - interstitial oxygen ($C_i O_i$) have been observed in most of the works [11,12] with hole traps at 0.23 eV and 0.36 eV respectively above valance band .

Table 1.1: Comparison of reported defect levels due to various ion in n-Si

Reference	Ions	O.V	$V_2^{-/-}$	$V_2^{-}/P.V$	Unknown(?)
Wang [28]	H^+, He^+, B^+, P^+	E(0.18)	E(0.23)	E(0.41)	
Troxell [21]	H^+, B^+, Si^+	E(0.16)	E(0.23) *3×10^{-16}	E(0.43) 2×10^{-15}	
Hallen [22]	H^+, He^+	E(0.18) 23×10^{-15}	E(0.24) 2.6×10^{-15}	E(0.42) 1.7×10^{-15}	E(0.32), E(0.45) E(0.5)
Svensson [20]	H^+, He^{2+}, O^{4+} S^{7+}, Br^{8+}, I^{10+}	E(0.17) 2×10^{-14}	E(0.23)	E(0.42) 2×10^{-15}	E(0.35)
Palmetshofer [23]	H^+, D^+ He^+	E(0.17) 8×10^{-15}	E(0.21) 1×10^{-16}	E(0.41) 2×10^{-16}	E(0.30), E(0.35) E(0.39)
Indusekhar [24]	He^{2+}	E(0.18) 1.2×10^{-15}		E(0.48) 5.3×10^{-13}	E(0.28) E(0.51)
Krynicki [25]	C			E(0.41)	E(0.63)
Mary [26]	U	E(0.17) 2×10^{-14}	E(0.22) 7×10^{-16}	E(0.44) 7×10^{-15}	
Zafar [27]	He^{2+}	E(0.17) 2×10^{-13}	E(0.20) 2.2×10^{-13}	E(0.43) 3.4×10^{-15}	E(0.26),E(0.31) 1.7×10^{-14}
Benton [19]	Si^+	E(0.18)	E(0.23)	E(0.40,0.44)	

* Capture cross-section in cm^2

Electron - irradiated Silicon , a review from CORBETT AND WATKINS [13].

In 1961 , Corbett & Watkins [13] found two electron - spin -resonance spectra Si - J and Si - C in electron - irradiated silicon and attributed it to the divacancy center (V_2) . They interprete this spectra as arising from a singly positive and singly negative charge of V_2 , respectively No resonances were observed in low resistivity n -type material indicating that V_2 may appear in four different charge states (+,0,-,2-) which was confirmed by a variety of experimental techniques , e.g., EPR[5] , IR[6] and DLTS [9,10]. The following level scheme has been proposed fro the DLTS studies[7,8], E_V + 0 25 eV V_2 (0/+ ; of charge state 0 if the level is occupied by an electron , + if unoccupied), E_C -0 42 eV V_2 (-/0); and E_c-0 23 eV V_2(2-/ -) where E_V and E_C represent the valance band and the conduction band respectively For electron - irradiated samples a close one - to - one relationship between the strengths of the levels E_C - 0 23 eV and E_C - 0.42 eV has been found in DLTS studies [9,10] Recent results shows that for MeV proton- and α- bombarded p^+-n diodes reveal a dose dependence for these two samples and a linear correlation does not hold for these samples [14].

Proton - irradiated Silicon , a review from PALMETSHOFER & REISENGER [15].

Proton bombardment of silicon has been studied for many years because of the importance in hydrogen in silicon technology as well as for the fundamental investigation of defects DLTS study reveals three vacancy related defect levels which have been studied originally in electron - irradiated silicon., in addition to it an additional defect level E_C - 0.30 eV was also observed which is the most prominent one . They studied the defect profiles of H^+ implanted silicon samples with different oxygen content and different phosphorous doping and found that the concentration of vacancy- related defects is independent of oxygen content , but linearly depend on the position of the Fermi level . Also found the defect profiles to be broader than the theoretical vacancy distribution which was explained by electric - field - enhanced diffusion . Recently , Hallen et al. [16] irradiated silicon at room temperature with 1.3 MeV protons using a dose of only $5*10^9$ cm^{-2} and dose rates of 10^7 to 10^{10} cm^{-2} s^{-1} . In direct contrast to the results for heavier ions and higher doses and dose rates , they

found a reverse dose rate dependence; i.e., for a constant dose the resulting defect density decreased with increasing dose rate

The above section gives a brief coverage of the work done with electron and proton bombardment and also with other heavier ions . The following section is specifically devoted to the literature survey related to our work .

1.3.2. Defects induced by He^+ ions : A Brief Review

It is well known that bombardment of silicon with light ions introduces defect states into the energy gap The primary point defects produced by the ion bombardment form complexes with other defects or with impurity atoms When the ion is chemically inactive as is He in silicon , one expects only pure damage related defects caused by primary or secondary displacement cascades [7] Early work on alpha particle irradiation was done primarily to compare effect due to electron and proton irradiation with that of He^+ Kimerling [7] in late seventies showed that the point defects character predominates even when silicon is bombarded with MeV alpha particles Since then several workers [8,9,17] have tried to catalogue the list of point defects produced by alpha particles through their electrical signature controlled by energy and capture cross section

The defects created by very low dose of alpha particles ($<10^{10}$ cm^{-2}) are studied by Kimerling [7] , and Berman et al [18] Infact , this study of low dose is common to almost all studies . The defects levels were characterized by DLTS technique [19] and the spectroscopy data reveals three dominant defect levels same as in electron - irradiated n -type silicon These levels have been identified as the oxygen - vacancy pair (O - V) for E (0.17) , the divacancy center (V -V) for E(0 21) and as a mixture of divacancy and the phosphorus - vacancy pair for E(0.41) [3,12,19] The vacancy - oxygen center (A-center) is fairly well understood defect [20,21] with an acceptor level at E_C -0.17 eV and its introduction rate is dependent on oxygen content of the sample . In crucible grown crystal the oxygen incorporated during growth produces large amount of this center . Even for float zone material , it has been shown

[7] that the oxygen incorporation during device fabrication steps is enough to give detectable levels of A-centers . This defects is formed when a vacancy is trapped by an interstitial oxygen atom . A characteristics of this center is that it can be annealed out at 400°• C , though its stabilization by forming complexes at higher temperatures have been reported at much higher temperatures . This trap level exhibits a very huge capture cross-section for electrons , $\sigma_n \sim 1*10^{-14}$ cm^2 [20]. The oxygen vacancy pair has been reported stable upto ~ 350° C [20].

The defect levels at E_C -0.23 eV and E_C -0.41 eV have been attributed to different charge states of divacancy [3] The former is associated with transition from double negative charge state to singly charged state , and the latter one with a further emission of an electron to become neutral The vacancy - phosphorus (P-V) center is a well understood defects and have capture cross-section ~ 10^{-15} cm^2 The E-center has been shown to have a charge-state dependent annealing [22]. Usually a it has been seen that in a DLTS spectra , an E-center related peak is overlapped by the presence of V_2^- related peak as they have similar trap parameters The overlapping nature of two peaks in DLTS has been a source of controversy as regards to concentration of two levels . However , differences in annealing behavior is used to differentiate between divacancy peak and E - center .

Recently this correlation has been studied in more detail by Svensson et al [9]. In their work they have irradiated high-purity n-type silicon samples with a series of high energy particles starting from light particles to very heavy MeV ions (electron, $^{H+}$,He^{2+},O^{4+},S^{7+},Br^{8+} , and I^{10+}) , and the two divacancy - related acceptor levels ~ 0.23 and ~ 0.42 eV below the conduction band (E_C) , respectively have been studied in detail using deep-level transient spectroscopy . They found that the concentration of two levels do not show one to one correspondence in many cases Though the concentration of the two levels are same in electron irradiated material , their ratio was dependent on depth in case of ion bombardment Depth concentration profiles show identical values for the two levels at shallow depths , while in the region close to damage peak large deviations from one- to- one proportionality are found . And also found that the deviations increases with ion dose and also hinge strongly on the density

of energy deposited into elastic collision per incoming ion . From the depth profile study it was concluded that the concentration of level corresponding to E_C -0.42 eV is significantly larger than that of E_C -0.23 eV level in regions of larger damage most probably due to strain favoring one state over the other . The E_C -0.42 eV peak in DLTS studies seemed to be broader for increasing projectile mass This was explained by a model which invokes motional averaging and lattice strain of the two states at higher temperature Further , the identification of E_C -0.41 eV is sometimes attributed to another defect due to donor -vacancy complex [3]. Their have been reports of additional defect levels without nailing down their origin [13,23].The occurrence is attributed to dose , introduction rate and the quality of the starting material Hence their has been differences in the energy spectrum reported by different workers .

The depth profile of defects produced by high energy He^+ ions have been critically studied by PALMETSHOFER and Reisinger [8] They studied the defect levels produced by H^+ , D^+ and He^+ bombardment of silicon with different phosphorus doping and oxygen content using transient capacitance spectroscopy They compared the profiles obtained with H^+ and D^+ ions and show that α-particles irradiation causes additional hydrogen related defects The defect profile investigation show that the maximum concentration of various defects occurs approximately at the projected ion range . However , found that the width of the defect profile is strongly dependent on the doping concentration and argue that broadening of the profiles , compared to theoretical distributions occur due to electric field enhanced diffusion . According to their argument such broadened profiles would not occur if irradiation are done within the depletion layer of a Schottky diode .

High fluences studies by Indusekhar et al [17] have used high energy (30 MeV) ,so that the particles escaped the silicon samples after traversing full thickness .Hence though they used large doses , the effective introduction rate of defects was small yielding results comparable to low doses .Therefore most of the studies report only small concentration of defects produced and use low background doping to increase sensitivity of detection

There has been very few studies on p - type Si compared to n - type Si . In a recent work , new metastable defect Hα2 in p - Si following room temperature alpha particle irradiation has been detected [24] DLTS measurements coupled with bias-on/bias-off cooling cycles were used to study the annealing introduction kinetics of this metastable defect .The energy level and apparent capture cross -section , as determined by DLTS , were E_V +0.43 eV and $1.4*10^{-15}$ cm^2 , respectively .

In order to encapsulate things ,it can be said that standard vacancy related defects appearing due to low fluences of alpha particles are fairly well known .However there is a lack of studies with high dose and epitaxial layers The other damage related defect levels have not been even properly identified and thus much less understood .

1.4.MOTIVATION AND AIM OF THIS WORK

In view of increasing importance of understanding electrical effects due to damage created by MeV ions , our laboratory has initiated a program on understanding deep levels induced by such ions in silicon . Typically such a program requires elaborate sample preparation methods involving , apart from modification , steps such as cleaning of wafers, contact formation ,Schottky barrier preparation and packaging of the sample . All these preparation methods require very controlled industry standard processing facilities . Furthermore the danger of incorporating process induced defects and their interaction is also quite high . While such studies are currently underway , several difficulties are encountered in obtaining reliable sample processing conditions It would be both convenient and scientifically interesting as well if one could use finished devices prepared commercially An attractive sample geometry suitable for these studies is a photodiode . The samples are easily available in packages suitable for irradiation in as received state with proper front and back back bonding and convenient transparent metallization on top . The sample configurations of photodiodes are also very simple with either metal - semiconductor contacts or p-i-n structure . In either case MeV ions would be penetrating up to the homogeneous semiconductor , and the structure is highly suitable for space charge layer based characterization techniques

such as deep level transient spectroscopy (DLTS) and time analyzed transient spectroscopy (TATS).

With this in mind , we set out to study effects of MeV ions in commercially available photodiode . Apart from this feasibility study , of great technological importance and scientific interest from the point of view of their use as photodetectors in space , and in high energy particle detectors in nuclear laboratories .

Since this was the first study in this direction in our laboratory the emphasis was on to find out experimental difficulties and advantages in using these photodiodes as work horse samples . Therefore we chose He^+ ions for this work recently on deep levels introduced by MeV alpha particles so that the traps induced would be easily identifiable standards Nonetheless the effect of He^+ particles is nearly intrinsic material such as used in photodiodes has not attracted enough attention .

A large area $1mm^2$ pin diode housed in a TO - 5 package with quartz window was chosen for the study . The sample was studied before and after irradiation of low dose ($1*10^{10}$ cm^2) He^+ ions with energy 1.26 MeV The characterization techniques mainly used were capacitance - voltage characteristics , deep level transient spectroscopy , thermally stimulated capacitance , and time analyzed transient spectroscopy . To be able to detect both minority carrier traps , the existing facility for these characterization were argumented with the possibility of optical filling pulses .

The results bring out the extent of feasibility , and differences in irradiation induced effects in the intrinsic silicon of a finished photodiode .

CHAPTER 2

PRINCIPLES OF EXPERIMENTS

2.1INTRODUCTION

This chapter is devoted to brief explanation of principles of various experiments used in this work . There are excellent reviews of this material in the literature [19,25,26] and we only approach a thumbnail sketch appropriate for this work and as much necessary for the discussion of results

2.2.CAPACITANCE SPECTROSCOPY

One of the most significant advances in recent years stems from the development of sophisticated techniques of monitoring the charge density and its changes in depletion layers. The capacitance spectroscopy ,in particular capacitance transient spectroscopy has furnished detailed information on deep traps The techniques consists of evaluating time- and temperature- dependent changes in the value of a capacitor which is formed by a depletion layer in a material with deep traps

This section presents a cursory glance at the many ways of measuring properties of deep impurities ,which emphasize the power of capacitance based characterization in conjunction with other electrical and optical techniques.

2.2.1.CAPACITANCE CHARACTERISTICS

2.2.1.1.Capacitance - Voltage Characteristics

The capacitance - voltage (C-V) technique relies on the fact that the width of a reverse biased space - charge region of a semiconductor junction device depends on the applied voltage.The scr width dependence on voltage lies at the heart of the a semiconductor junction device depends on the applied voltage. This scr width

dependence on the voltage lies at the heart of C-V technique. The C-V profiling method has been used to determine the carrier concentration of the sample

A depletion layer as shown in Fig 2 1. establish due to the built - in voltage (V_b) and applied voltage (V_a) . Then the electron density distribution can be given by n(x) at the edge of depletion region . This charge distribution can be given electron in metal and positive charge in semiconductor as

$$d^2\psi/dx^2 = -\rho(x)/\varepsilon\varepsilon_0 \quad \text{---------- 2.1}$$

where ρ(x) is the charge density obtain from the charge distribution profile. In metal as charge is small compared to semiconductor hence solution of the above equation can be given by

$$\psi(x) = ((x_d - x)^2 eN_d)/2\varepsilon\varepsilon_0 \quad \text{---------- 2.2}$$

where x_d is the depletion width Then the electron distribution in this region is given by

$$n(x) = N_d \exp\left[-(x_d - x)^2/2L_d^2\right]^{1/2} \quad \text{---------- 2.3}$$

where $L_d = \left(\varepsilon\varepsilon_0 kT/e^2 N_d\right)$ is called Debye length.

2.2.1.2.Capacitance - Voltage Profiling

Assuming the semiconductor (Schottky diode) to be an ideal capacitor and depletion approximation is valid , provided there is no influence of deep states , the doping concentration can be calculated as given below.

Consider the semiconductor to be n-type with doping concentration N_d .A dc bias V is applied to the metal contact. The reverse bias produces a space-charge-region of width x_d .The capacitance is defined by

$$C = \frac{dQ}{dV} \quad \text{---------- 2.4}$$

where Q is the semiconductor charge. The capacitance is determined by superimposing a small - amplitude ac voltage v on the dc voltage V.

A dc voltage V plus a sinusoidal ac voltage v is applied across the semiconductor diode. The ac voltage increasing form zero to small positive voltage adds a charge increment dQ_m to the metal contact (shown in Fig 2.2).The charge increment dQ_m is balanced by an equal semiconductor charge increment dQ for overall charge neutrality, where

$$dQ = -qAN_d(x_d)dx_d \quad \text{---------- 2.5}$$

The charge dQ , as shown in Fig.2.3 , comes about through a slight increase in the scr width .So, putting equation 2.5 in equation 2.4 we get ,

$$C = \frac{dQ}{dV} = -qAN_d(x_d)\frac{dx_d}{dV} \quad \text{---------- 2.6}$$

The capacitance of a reverse - biased junction , when considered as a parallel plate capacitor , is expressed as

$$C = \frac{K_s\varepsilon_0 A}{x_d} \quad \text{----------2.7}$$

Differentiating the above equation with respect to voltage and substituting dx_d/dV

we get

$$N_d(x_d) = -\frac{C^3}{qK_s\varepsilon_0 A^2\left(dC/dV\right)} \quad \text{---------- 2.8 (a)}$$

which can also be written as

$$N_d(x_d) = \frac{2}{qK_s\varepsilon_0 A^2\left[d\left(1/C^2\right)/dV\right]} \quad \text{---------- 2.8 (b)}$$

The doping concentration is obtained from a C - V curve by taking the slope dC/dV or by plotting $1/C^2$ versus V and taking the slope $d\left(1/C^2\right)/dV$ .The depth at which the doping concentration is evaluated is obtained from equation 2.8 .In deriving the equation (2.8), we used the depletion approximation which completely neglects minority carriers and assumes total depletion of majority carriers in the space-charge-region to a depth x_d and perfect charge neutrality beyond x_d .

This method of non destructive profiling is limited by (1) fundamental , (2) instrumental, (3) sample limitation. The reverse breakdown field decides the maximum depth in a sample .

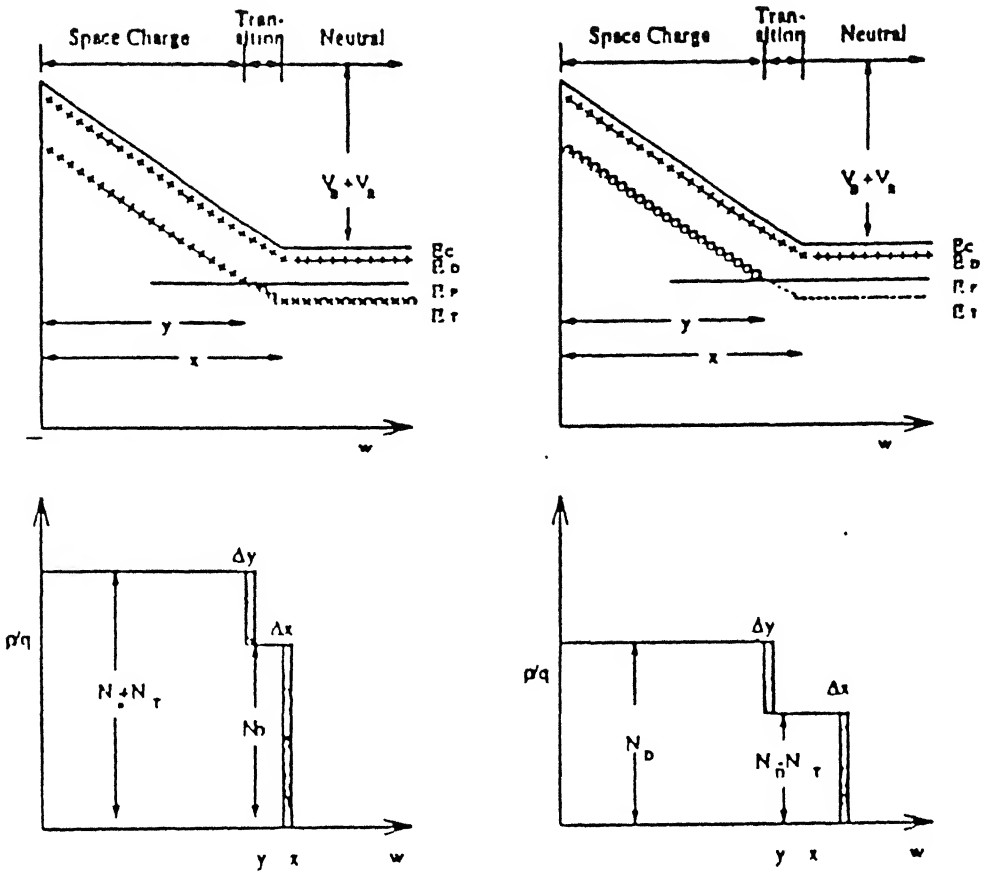

Fig.2.1. Band bending diagram in reverse condition .

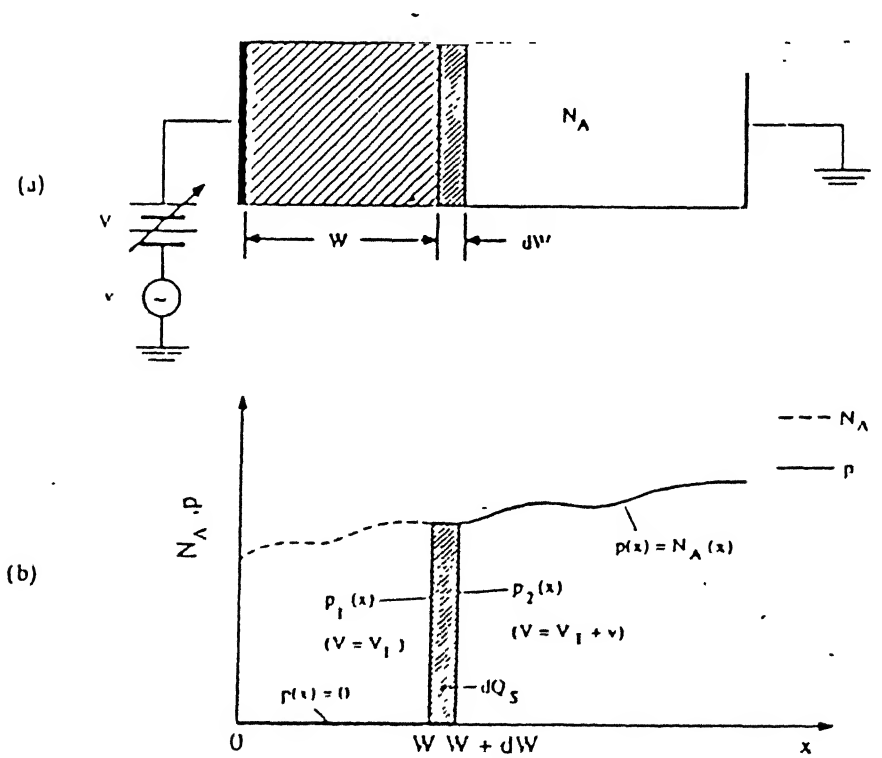

Fig.2.2. The doping concentration and majority carrier profiles in the

A lower doped sample will have a higher depth . Depth resolution can be represented by $\cong x_d \pm L_d$ .Further difficulties arises due to diffusion of free carriers. Gradient of concentration, established charge dipole within undepleted material and as the depletion layer of the surface contact approaches the depletion layer of the surface contact approaches redistribution of charge occur.

It is difficult to achieve a satisfactory balance between optimum depth resolution and accuracy in measurement of N in the depletion profiling and this arises from coupling between Δx_d , $N(x_d)$ and depth Presence of deep states in the material introduces distortion in a C-V profile . Also the presence of series resistance and leakage in the test diode introduces distortion in C-V profile.

2.2.2.TRANSIENT CHARACTERISTICS

The characterization of deep level defects are best measured electrically by transient study at various temperatures.

2.2.2.1.Transient Measurement

Fig.2.3 shows the change in space charge region width x_d as electrons are emitted from G-R centers.In transient measurement it is time-varying capacitance which is given by

$$C = A\left((qK_S\varepsilon_0 N_d)/2(V_{bi} - V)\right)^{1/2}\left(1 - \left(n(t)/N_d\right)\right)^{1/2}$$

$$\cong C_0\left(1 - \left(n(t)/2N_d\right)\right) \text{ ---------- 2.9}$$

where C_0 is the capacitance without any deep level impurities at reverse bias - V. In most of the cases it turns out that deep level impurities form only a small fraction of the space-charge-region impurity concentration or $N_t << N_d$ which gives

$$C = C_0\left(1 - n_t[t]/2N_d\right) \text{ ---------- 2.10}$$

The above equation is only valid for low impurity concentrations.

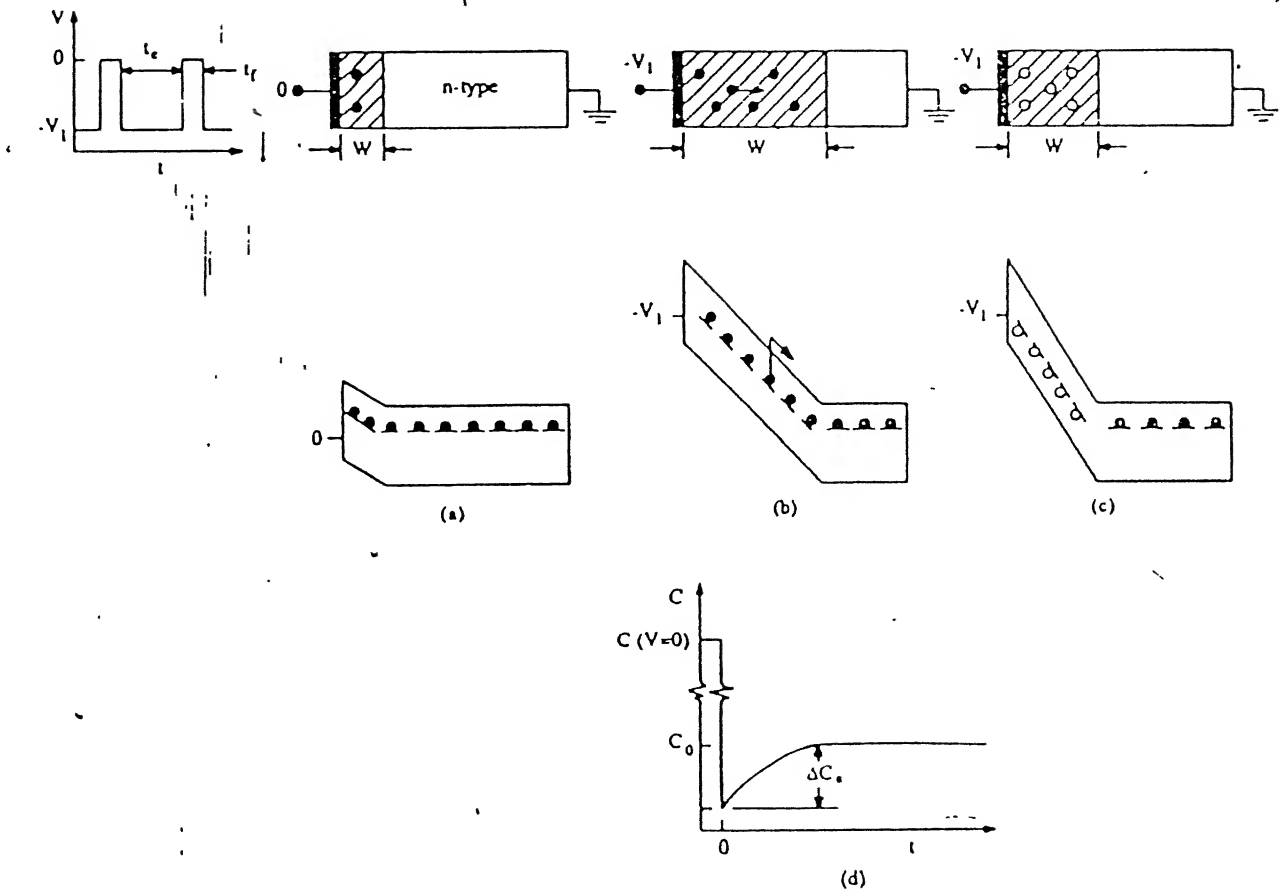

Fig.2. 3 A Schottky diode for (a) zero bias (b) reverse bias at t=0 (c) reverse bias as $t \to \infty$ (d) the capacitance transient .

The most common measurements are emission measurements. The junction device is initially zero biased , allowing impurities to capture majority carriers. Following a reverse bias pulse , majority carriers are emitted as a function of time (shown in Fig.2.3 (a)) . The capacitance during this time is given by

$$C = C_0\left[1 - \frac{n_T(0)}{2N_d}\exp(-t/\tau)\right](t > 0) \quad \text{----------} \quad 2.11$$

where C_O is steady state capacitance value at reverse bias , n_T is occupied trap concentration and N_d is shallow doping concentration , and τ_e is the characteristics emission time constant of the trap.

Immediately after the device is reverse biased the space-charge-region is widest and the capacitance is lowest But as the majority carriers are emitted from the G-R centers (shown in Fig.2 3 (b)) , x_d decreases and C increases until steady state is attained (shown in Fig.2.3 (c)) The same time dependence of the capacitance is observed for deep level donor impurities in n-type substrates . Here both charge and capacitance increases with time regardless whether the deep-level impurities are donors or acceptors. This also remain true for p-type substrates with either donor or acceptor G-R centers .The capacitance increases with time for majority carrier emission .

From decay time constant of the C-t curve , τ_e is derive , and from the reverse-biased capacitance change $n_T(0)$ is obtained Defining

$\Delta C_e = C(t=\infty) - C(t=0)$, we have

$$\Delta C_E = \frac{n_T(0)}{2N_d}C_0 \quad \text{----------} \quad 2.12$$

Plotting the capacitance $C(\infty) - C(t) = \frac{n_T(0)}{2N_d}\exp(-t/\tau)$ as ln $\left[C(\infty) - C(t)\right]$ versus t , a slope of $-1/\tau_e$ and an intercept on the ln axis of $\ln n_T(0)C_0/2N_d$ is obtained which gives information about the trap parameters The emission time constant τ_e in the equation has an Arrhenius dependence on temperature given by

$$1/\tau_e = \sigma_n < v_{th} > N_c \exp\left(-\frac{E_T}{kT}\right) \quad \text{----------} \quad 2.13$$

where E_T is the activation energy of the trap and σ_n is the capture cross section of the trap. Thus monitoring of capacitance transients at various temperature allows determination of τ_e as a function of temperature and hence trap parameter extraction E_T and σ_n . Details of C-t measurement method can be found in [27].

2.2.2.2.Deep Level Transient Spectroscopy

Though several methods are known for extracting time constant from capacitance transient directly , the advantages of spectroscopy in transient analysis was first realized by D V Lang [19] This is a high frequency capacitance transient thermal scanning method useful for observing a wide variety of traps in semiconductors The technique is capable of displaying the spectrum of traps in a crystal as positive and negative peaks on a flat baseline as a function of temperature. It is a sensitive technique , which is rapid and easy to analyze. The sign of peak indicates whether the trap is near the conduction band or valance band , the height of the peak is proportional to the trap concentration ; and the position , in temperature , of the peak is determined by the thermal emission properties of the trap . Even the activation energy , concentration profile , and electron- and hole- capture cross sections for each trap can be obtained from this.

The physics of DLTS is in the capacitance transients . The essential feature of DLTS is the ability to set an emission rate window such that the measurement apparatus only respond when it sees a transient with a rate within this window . Thus , if the emission rate of a trap is varied by varying the sample temperature , the instrument will show a response peak at the temperature where the trap emission rate is within the window . These emission rates are thermally activated and by the principle of detailed balance it is found to be

$$e = < \sigma v_{th} N_d > \exp(-\Delta E/kT) \quad \text{---------- 2.14}$$

Many variants of the conventional DLTS have been purposed for characterization of semiconductor including frequency scanned DLTS , Fourier transform DLTS , optical and scanning DLTS , lock in DLTS , interface trapped

charge DLTS etc. In the next three section , we will describe a variant of three different DLTS technique which we have used extensively in our work .

2.2.2.2.1.Boxcar DLTS

The DLTS scheme presented here makes use of a dual - gated signal averager (double boxcar) to precisely determine the emission rate window and to provide signal averaging capability to enhance the signal - to - noise ratio for the detection of low concentration traps .

The use of double boxcar to select rate window is illustrated in Fig.2.5 The capacitance transients are observed in a capacitance meter A series of such of such capacitance transients for a typical trap at various temperatures is shown in schematically on the left hand side of Fig.2.5 .The emission rate is very small for low temperatures and becomes rapid as the temperature is increased . These transient signals are fed into a double boxcar with gates set at t_1 and t_2 as shown in Fig.2.5 The signal from the differential output of the boxcar is recorded This is simply the capacitance at t_1 , $C(t_1)$, minus the capacitance at t_2 , $C(t_2)$. The difference $C(t_1)$-$C(t_2)$, goes through a maximum when τ , the inverse of the transient rate constant , is on the order of t_2 - t_1 Thus , the values of t_1 and t_2 determine the rate window for DLTS scan .

Defining the normalized DLTS signal S(T) , as $S(T)=\left[C(t_1)-C(t_2)\right]/\Delta C(0)$ where $\Delta C(0)$ is the capacitance change due to the pulse at t=0 and for exponential transients we have

$S(T)=\exp(-t_1/\tau)-\exp(-t_2/\tau)$ where τ is related to temperature by the expression . The relationship between τ_{max} and t_1 and t_2 is simply determined by differentiating S(T) with respect to τ and setting the result equal to zero . Thus

$$\tau_{max}=(t_1-t_2)\left[\ln(t_1/t_2)\right]^{-1} \quad \text{----------2.15}$$

At the maximum of the DLTS signal , measuring τ_{max} and the temperature we can generate the Arrhenius plot (1000/T Vs. $\ln(\tau T^2)$) from which activation energy

and capture cross section can be calculated . The trap concentration can be obtained from the DLTS peak height which is given by

$$N_T = (\Delta C_{max}/C_0)2N_d\left(r^{r/r-1}/1-r\right) \text{ where } r = t_2/t_1 \text{ ---------- 2.16}$$

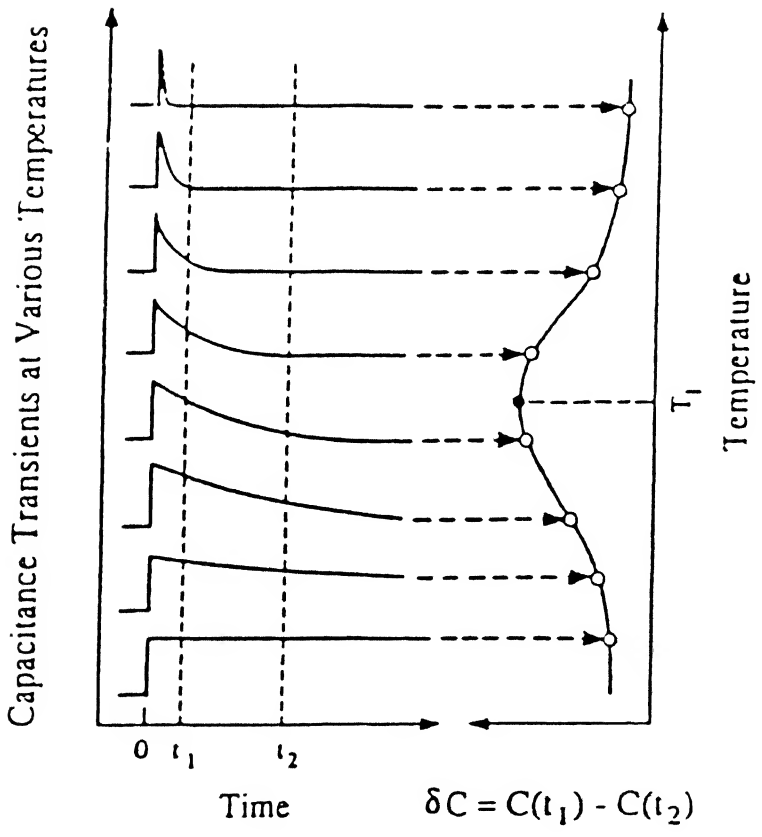

Fig.2.5. Transient emission rate and construction of Boxcar signal .

2.2.2.2.2 Optical DLTS

Optical DLTS comes in various implementations . Light can be used

- to determine optical properties of G - R centers , such as optical capture cross sections ,
- to create electron - hole pairs for minority carrier injection ,
- to create electron - hole pairs in semi - insulating materials , where electrical injection is difficult

Traps are detected as light imparts energy to the trap carriers causing its emission from a G - R center to the conduction or to the valence band , and it changes n and or p by creating electron - hole pairs , thereby changing the capture properties of the center.

Although optical DLTS can be done in several ways , the optical DLTS technique which we have used in our work uses an infrared LED Here variable energy probe light excites carriers from the traps into either of the band while the junction is pulsed electrically Both the electrons and hole can be captured by traps in the space - charge - region .When the light is turned off , the carriers are thermally emitted . In this method the light is merely used to generate electron - hole pairs ; the transition is due to thermal emission .

As purely electrical measurements are difficult to do in high resistivity or semi - insulating substrates . Optical inputs can then be a decided advantage and in some cases are the only way to obtain information on deep level impurities .

2.2.2.3.Time Analyze Transient Spectroscopy (TATS)

Unlike DLTS , here the time window is varied keeping the temperature constant [28] . It is an isothermal spectroscopic technique based on difference signal in time window . The TATS signal is given by

$$S(t) = C(t,T) - C(t+\gamma t, T) \quad \text{---------- 2.17}$$

where C represents isothermal capacitance transient at temperature T and γ is an experimental chosen constant . For exponential transient of time constant τ_e , S(t) has a maximum when plotted against ln(t) and maximum occurs at time t_m given by the relation

$$\tau_e = \frac{\gamma t_m}{\ln(1+\gamma)} \quad \text{---------- 2.18}$$

The peak value of the TATS signal is given by

$$S_{max} = C_0 \frac{N_T}{2N_d} \frac{\gamma}{1+\gamma} (1+\gamma)^{-1/\gamma} \quad \text{---------- 2 19}$$

where C_0 is the prefactor of the transient C(t , γ)

TATS has several advantages over DLTS .As it is spectroscopy in time domain alone , therefore possible temperature dependence of the transient prefactor containing occupancy etc. does not occur Besides this the line shape analysis in TATS does not depend on trap parameters as in DLTS

2.2.2.4.Thermally Simulated Capacitance (TSCAP)

Another technique which also gives information regarding defect levels in a semiconductor is TSCAP . This technique was used before DLTS became popular . During the measurement the device was cooled under either reverse bias And after cooling , a short filling pulse is given to filled the trap with majority carriers . Alternately , traps can be filled with minority carriers by optical injection or by forward biasing the device Then the device is reverse biased , heated at a constant rate , and the steady capacitance is measured as a function of temperature . Capacitance steps are observed as traps emit their carriers .

The temperature T_m corresponding to the mid-point of TSCAP step is related to the activation energy ΔE by

$$\Delta E = kT_m \ln\left[\frac{\nu k T_m^2}{\beta(\Delta E + 2kT_m)}\right] \quad \text{---------- 2.20}$$

where β is the heating rate and γ is attempt to escape frequency . The step height of TSCAP curve gives the trap concentration . Activation energy can be obtain form the Arrhenius plot of $\ln(T_m^2/\beta)$ versus $1/T_m$ for varying heating rate (β) .The majority and minority carrier trap can be distinguished by noting the sign of capacitance change .

Thermally stimulated techniques allow a quick sweep of the sample and work well for $N_T \geq 0.1 N_d and \Delta E \geq 0.3 eV$ i.e its sensitivity is much less than the spectroscopic techniques described earlier In terms of convenience of use and interpretation , TSCAP is less convenient than DLTS and TATS due to requirement of controlled thermal scan rate.

CHAPTER 3

EXPERIMENTAL TECHNIQUES FOR ELECTRICAL CHARACTERIZATION

3.1.INTRODUCTION

The history of research in semiconductor physics and solid state electronics is filled with novel experimental techniques to control the concentration of the impurity and defect centers, to measure their electrical and optical properties and to physically understand and theoretically predict these electrical , optical as well as thermal properties. These impurities and defects are usually present in minute quantities in most practical situations. Thus, it becomes a major challenge to detect their presence and to measure their properties accurately

In this chapter we describe the experimental details of sample , set - ups used for its modification by MeV implantation and characterization techniques used .

3.2.ABOUT THE SAMPLE

As mentioned in the introduction , one of the chief goal of this study is to find out the feasibility of using a Si photodiode for MeV implantation studies . A commercially available pin photodiode (centronic) in a TO - 5 package was chosen for the study . The Si photodiode has an area of 3.14 cm^2 . The area of particle beam is also similar and hence uniformity of damage is easy to obtain The top cover of the TO - 5 package has a quartz window which was broken before irradiation .

3.3 He^+ ION IRRADIATION

High energy He^+ was used for implantation on the sample. He^+ ions of energy 1.26 MeV generated by the Van de graaff accelerator was used to irradiate the sample with dose $1*10^{10}$ ions/cm^2 . The beam spot on the sample was typically of 4 mm^2 as measured on paper . The irradiation was carried out at room temperature.

3.3.1.He^+ Ion Irradiation Port

The ion irradiation port is shown in Fig.3.1 .This chamber is mounted on a diffusion pump vacuum system. Such a vacuum system can provide vacuum upto 10^{-6} torr Care was taken to avoid carbon deposition on the sample during irradiation.

The sample was mounted on a sample holder . By moving the holder vertically by a predetermined amount the required sample was introduced in the path of the He^+ ion beam A Current integrator was connected to the sample holder which measures the total charge acquired during irradiation From the collected charge the dose (number of ions incident per cm^2) was calculated Surrounding the sample holder there was a cylinder made of aluminium sheet which has an opening for the passage of heavy ion beam. This arrangement is called a suppressor which inhibits the emission of secondary electrons from the sample during He^+ ion implantation.

The beam which enters the chamber was collimated by the X -Y slits. By the time it reaches the chamber it spreads slightly and is further collimated by an aperture, mounted just before the sample holder. The aperture can be adjusted for area up to 5×5 mm^2 .In the irradiation carried out the ion current density used , have energy 0 2 $\mu A/mm^2$. The He^+ ion irradiation was carried at an angle $0^{\circ\bullet}$ with a dose $1*10^{10}$ ions / cm^2 .

3.3..2 MeV Ion Facility

The 2 MeV Van de Graaff accelerator facility at IIT,Kanpur has been utilized in this work. The details about the accelerator has been described in Banerjee N [29] and Chauduri [30] .The schematic layout of the ion beam irradiator was shown in Fig.3 2.

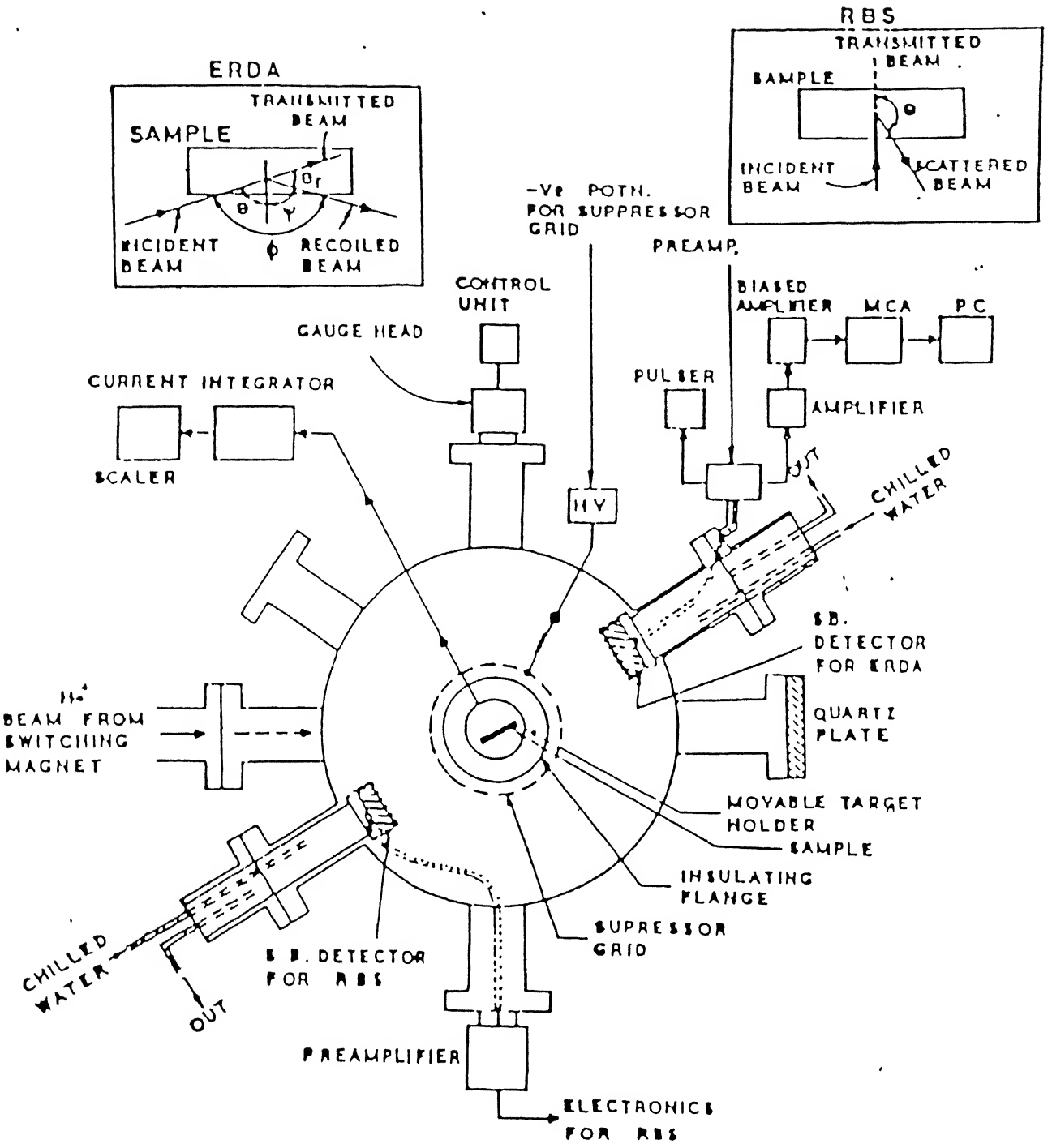

Fig.3.1. Block diagram of the chamber and associated electronics for RBS and ERDA measurements .

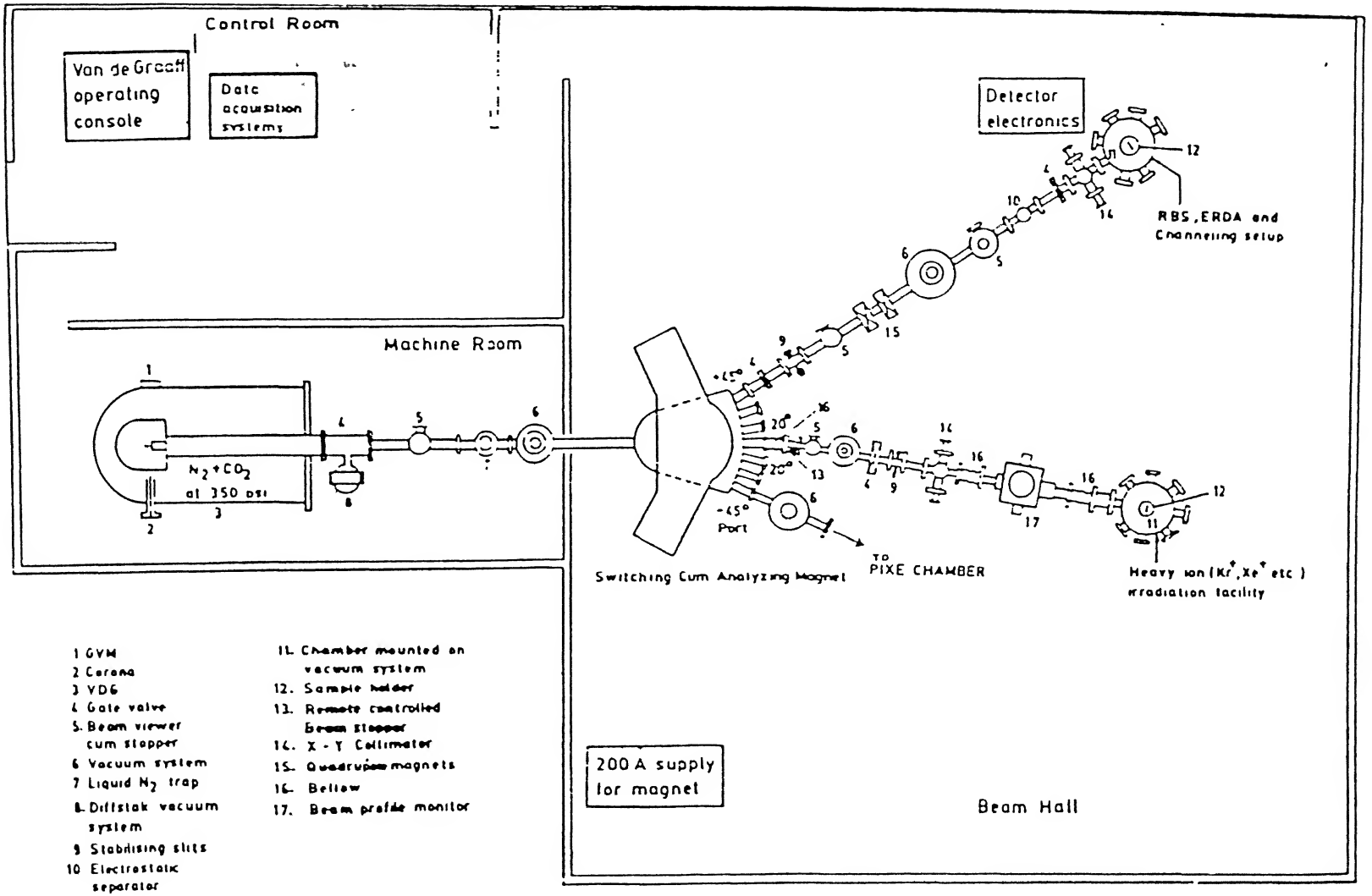

Fig.3.2. Lay out for accelerator set up .

.3.4 ELECTRICAL CHARACTERIZATION

This section gives a brief description about the various experimental techniques involved in electrically characterizing the sample. Basically,the electrical characterization involves the capacitance measurement as a function of temperature, time and voltage. The same setup was used for both the transient and steady state measurements. The whole setup was made computer controlled except for the temperature programming. A block diagram of the experimental setup is shown in Fig.3.3 .

3.4.1 EXPERIMENTAL DETAILS

3.4.1.1 Sample Temperature Measurement

All the measurements carried out in this work was performed in the temperature range 80K-300K The sample was mounted inside the conical shaped aluminium cryostat (shown in Fig. 3.4) which has a copper-constantan thermocouple.The design of cryostat was made so as to enable quick and easy change of sample for temperature control and scanning capabilities. A heater wire 30 V , 110 Ω with proper insulation is wounded on the bottom protruding portion of the aluminium block serving as the sample chamber and water-ice mixture is used as constant temperature reference. The thermocouple reference junction is kept in ice-water mixture(273 K) and the other junction is placed on top of the sample header. The copper-constantan thermocouple is fed to a GPIB controlled Keithley digital multimeter (Mode 196).The temperature is thus monitored on the screen by converting the thermocouple voltage into temperature using look-up tables in the computer programs.

3.4.1.2. Current - Voltage Measurement

For preliminary characterization a photo I - V measurement was taken The set up for it is shown in Fig 3.5. Here the sample was exposed to an infrared LED . Two sets of measurments were taken . One by varying the reverse bias voltage and then measuring the photo current , keeping the LED current fixed . Another by varying the

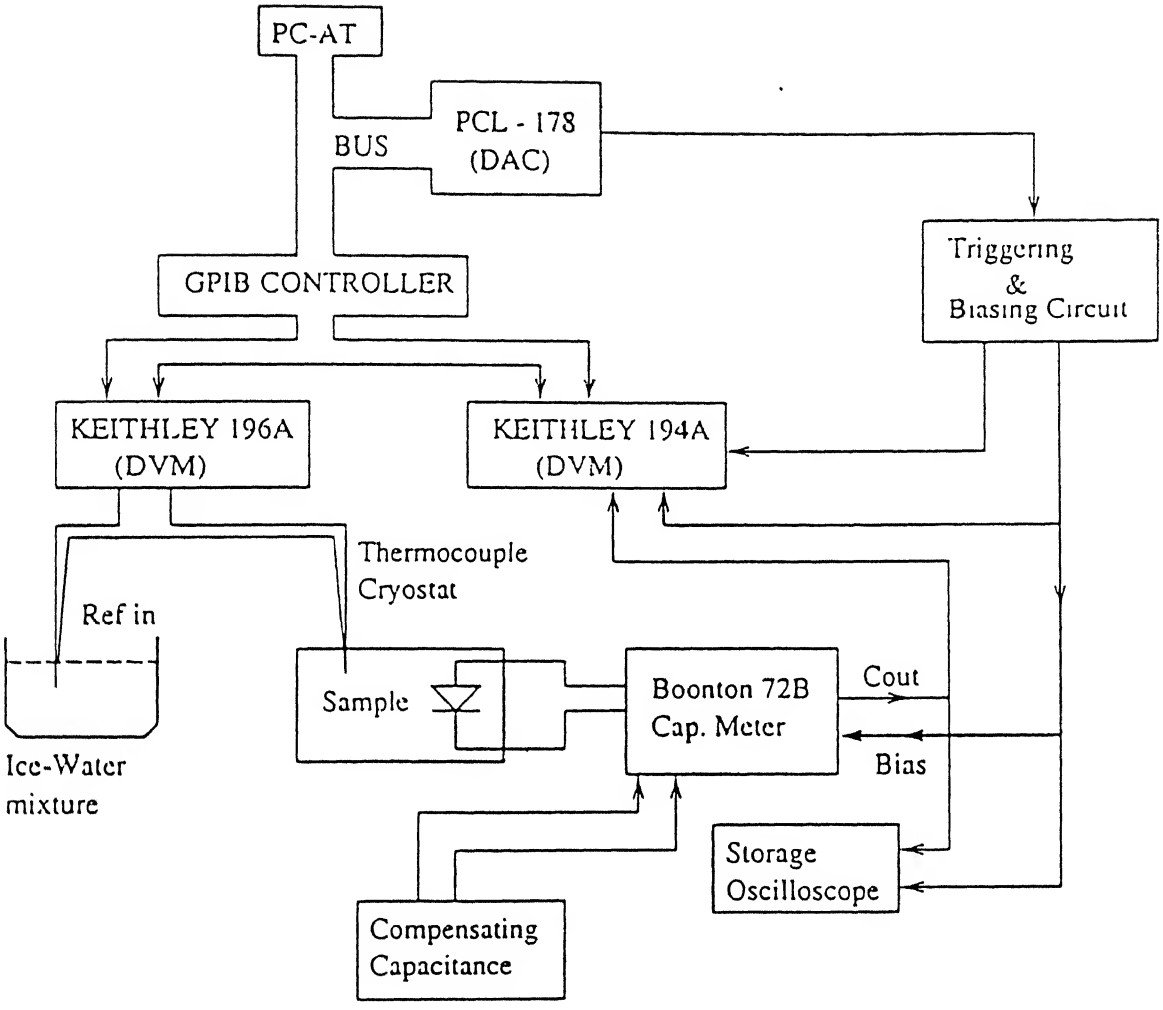

Fig.3.3. Block diagram of the capacitance/voltage transient and DLTS/TATS measurement system .

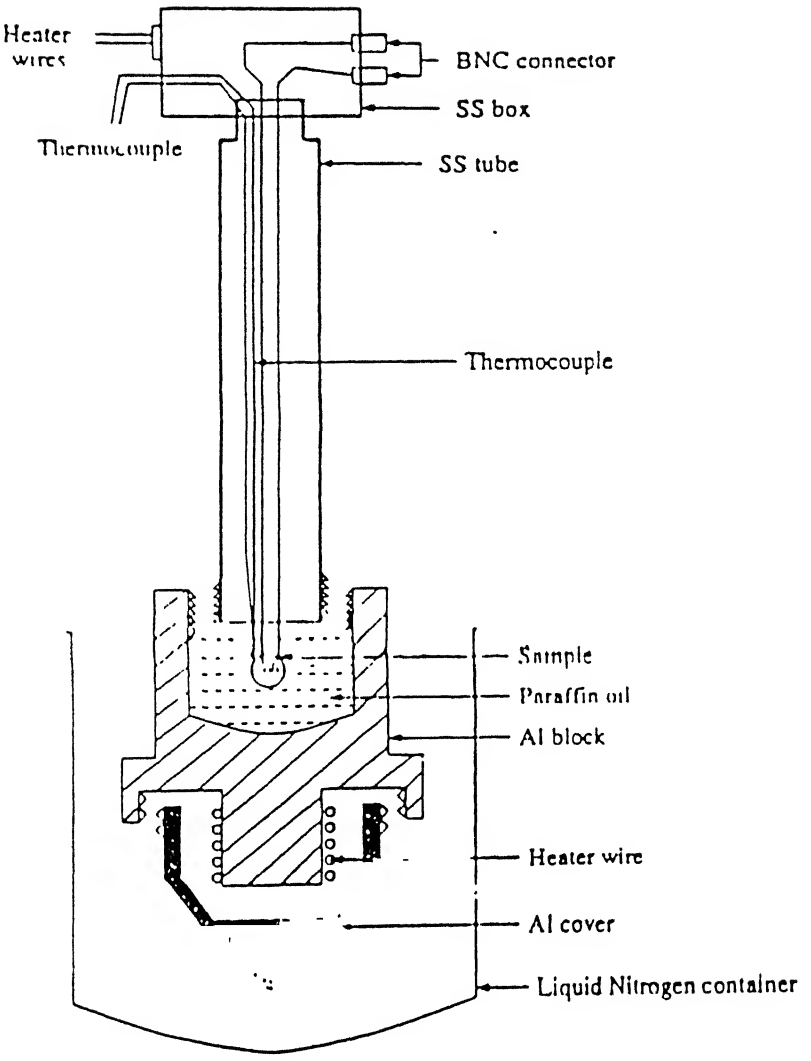

Fig.3.4. Schematic of cryostat (temperature measurement unit) .

LED current and measuring the forward current through the photodiode. Here the current was measured with digital multimeter.

3.4.1.3. Capacitance - Voltage Measurement

A Boonton capacitance meter (Model 7213 with 50 μsec response time) is used for all capacitance measurements. Its resolution is 0.5 % and frequency of the crystal is 1MHZ.

Programmable voltage is generated with the help of a plug-in AD / DA card (Model PCL 718).The card has two analog outputs (range 0 to +5 V, with a resolution of 12 bit and 5 μ sec settling time). For changing the polarity of the voltage, an Opamp inverting circuit is implemented as shown in Fig.3 6 .

The voltage was changed from high value to low value while monitoring the capacitance at each voltage. For all C-V measurements, voltage was swept at a predetermined rate from high voltage to low voltage and then from low voltage to high voltage. The sample was kept under reverse bias condition and both the applied voltage and capacitance meter analog output are digitized through the two input channels of Keithley high speed voltmeter (Keithley 194A) which can store 64 KB data. For C-V measurement, at first temperature was monitored and voltmeter was triggered (internal) to measure the applied voltage and capacitance simultaneously in two channels of the high speed voltmeter. The control was done through IEEE-488 interface bus.

3.4.1.4 Capacitance Transient Measurements

This was carried out by keeping the sample under reverse bias and the desired temperature was achieved through proper control of heater current in the cryostat and liquid nitrogen level. The bias voltage pulses and trigger pulses are generated from the PCL 718 card along with the help of a multiplexer.

The capacitance meter had a fast response time option of 50 μ sec installed in it. For obtaining the capacitance transients, the analog output of the capacitance meter was digitized using high speed voltmeter Keithley 194 A.

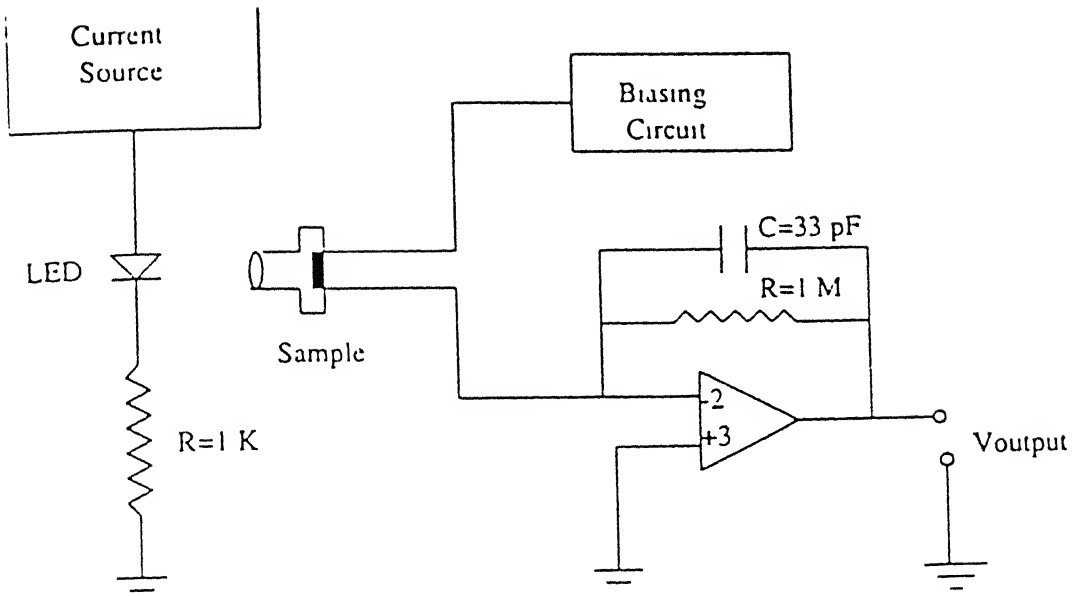

Fig.3.5. Schematic for current - voltage measurement .

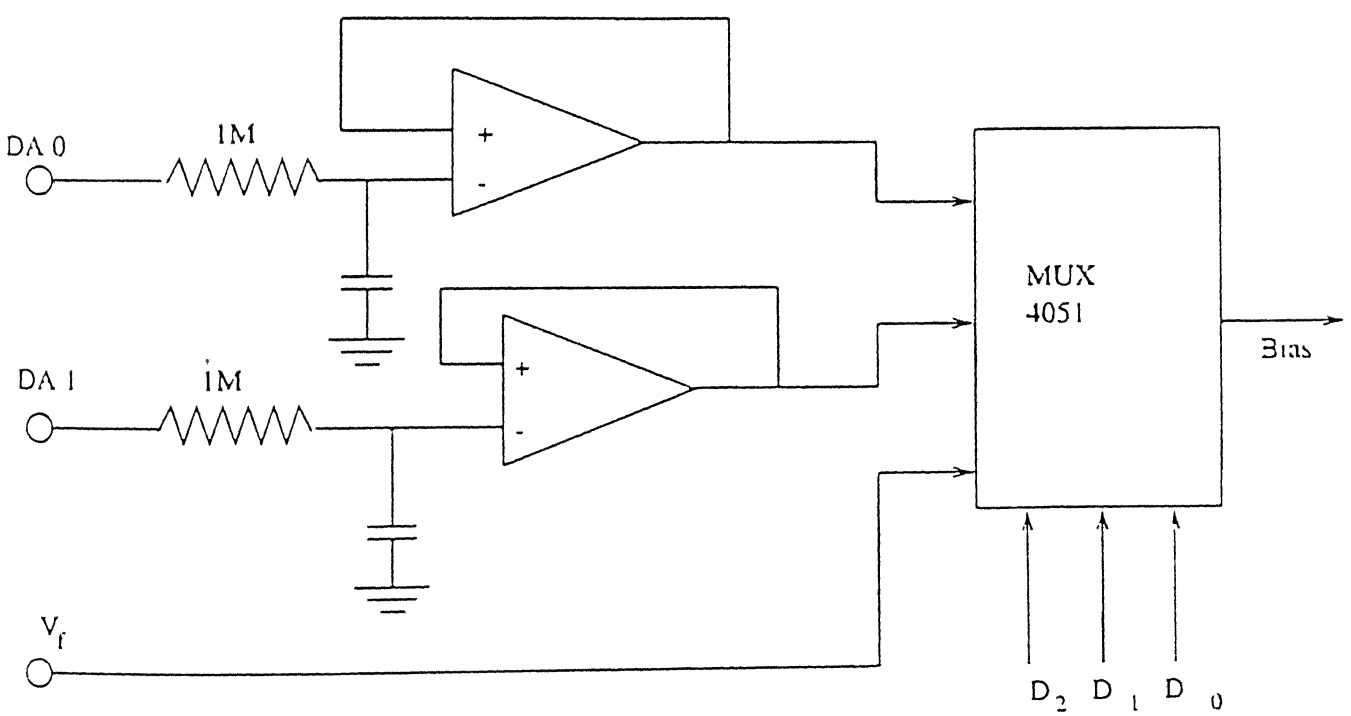

Fig.3.6. Schematic of bias and triggering circuit .

The following steps were involved for recording the capacitance transient.

- Sample was kept under reverse bias.
- Temperature was stabilized in the cryostat to the desired degree of accuracy.
- Filling pulse was applied .
- The high speed voltmeter (Keithley 194 A) was triggered for data acquisition at the end of fill pulse.
- The acquired data then transferred from Keithley 194 A to the PC for further processing .

3.4.1.5 Deep Level Transient Spectroscopy (DLTS) Measurements

The experimental setup involved in order to carry out deep level transient spectroscopy measurements is same as that shown in Fig.3 3 . The capacitance waveform (C-t) was digitized at each temperatures. Generally, a filling pulse of duration 50 msec was used in most of the DLTS measurements. The following steps were used in carrying out the measurement.

- The sample was cooled under reverse bias.
- After attending the lowest temperature (80 K), the temperature was increased slowly by adjusting the height of liquid nitrogen can and heater current.
- At each temperature 10 transients were taken and averaged in order to improve the signal to noise rate.
- The measurements were carried out for 7 different gates (rate windows) in a single scan for obtaining the Arrhenius plot.
- Various signal processing functions were performed on C-t data to improve signal / noise ratio.

This experiment is also referred as C-V DLTS as the voltage here was kept constant throughout the experiment.

3.4.1.6 Optical DLTS Measurement

This was done by employing the same setup as in C-V DLTS (shown in Fig.3 3). Beside here the sample was exposed to light. For this an additional circuitry was used to shone light on the sample as shown in Fig.3.7 . The steps involved are same as in C-V DLTS measurement technique . Here the sample was cooled under reverse bias and light was shone on the sample to fill the trap . The trigger (0-5 V) was also provided to the circuitry in order to pulse the light. A thin perspex hollow cylinder with holes at both ends for mounting the sample and LED was used

3.4.1.7. Time Analyzed Transient Spectroscopy (TATS) Measurement

This was done at a stabilized temperature by acquiring the entire transient (Ct) with 30,000 data points with typical sampling rate of 1 msec Data in logarithmic time was extracted after proper filtering. Transients at several temperatures were taken which can be used afterwards to get the Arrhenius plot. The measurements were carried out in both the conditions i.e., with the pulse trigger (0-5 V) and also with LED pulsing

3.4.1.7. Thermally Stimulated Capacitance (TSCAP) Measurement

In this measurement, the sample was cooled under reverse bias and at lowest temperature the traps are filled with majority carriers at zero bias or forward bias. Then again the reverse bias was applied , and heated at constant rate to monitor the steady state capacitance as a function of temperature The experiment was also carried out without giving the filling pulse at low temperature and used as reference for isolating capacitance changes due to trap emission.

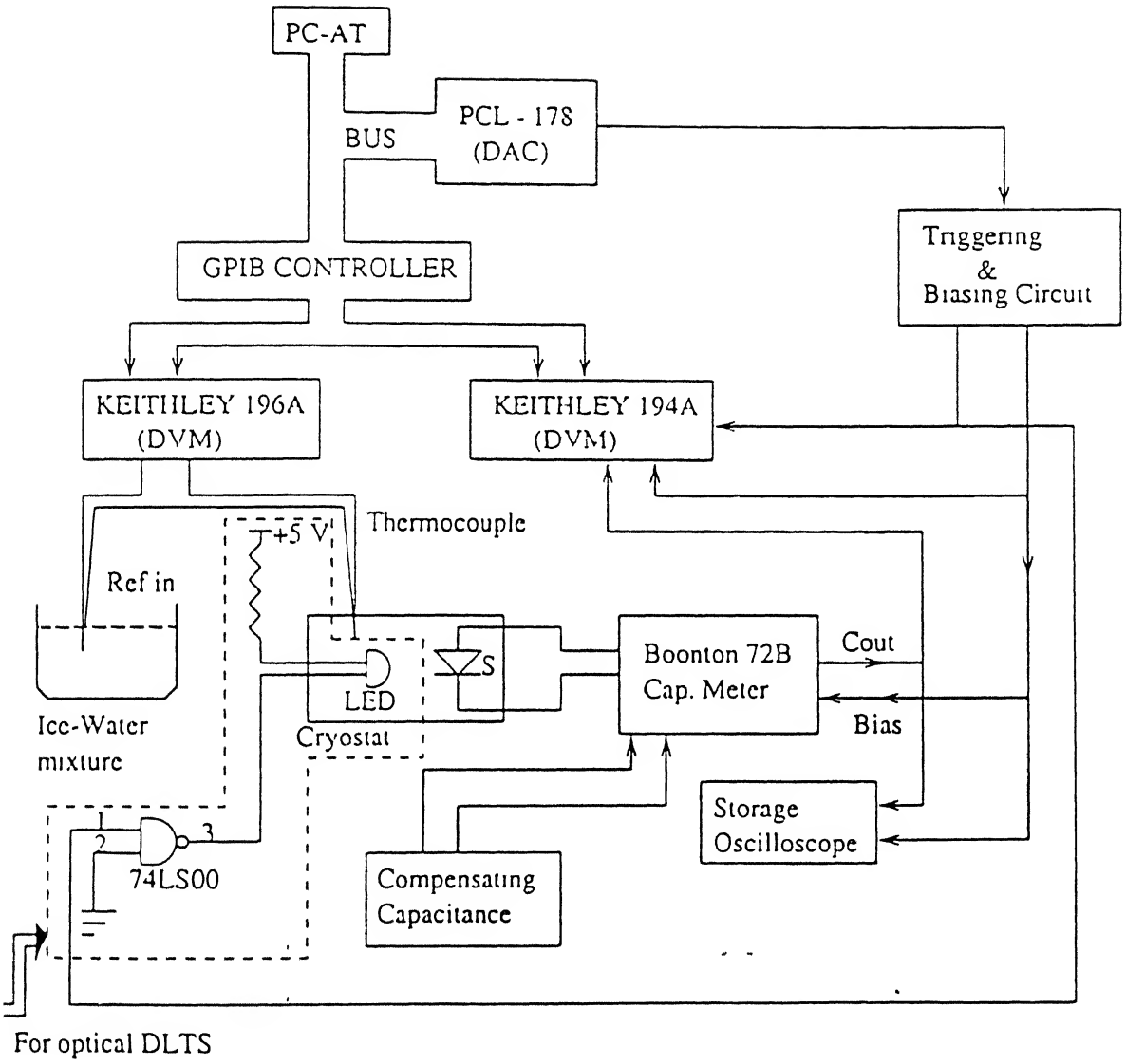

Fig.3.7. Block diagram for optical DLTS measurement set up .

CHAPTER 4

RESULTS AND DISCUSSION

As pointed out in chapter 1 , our major goal is to study feasibility of using commercially available photodiodes for MeV particle radiation , and to characterize in the process defects created by MeV alpha particles in standard photo detectors We first give measured standard characteristics of photodiode . In the second half we focus on characterization of irradiation induced deep levels in the sample .

For convenience of discussion , we briefly recall the sample details The sample is a commercial fast photodiode with the active layer being intrinsic We try to look for presence of deep traps before irradiation and then again do so after irradiating a low dose of $1x10^{10}$ cm^2 of He^+ ions with energy 1.26 MeV .

4.1. Measurement of Sample Characteristics

The sample being a photodiode ,we first show I - V characteristics of the sample under photoexcitation . An infra-red forward biased LED is mounted in front of the sample to measure these characteristics . A typical plot at room temperature is shown in Fig.4.1. Note that the reverse current is indeed high and constant over the whole range of reverse bias up to -10 V as expected for a decent photodiode. Fig.4.2. shows the photocurrent at a reverse bias of 9 V as a function of forward current in the LED . Assuming that LED light output is linearly proportional to the forward current , the photodiode response is also linear . These characteristics are insensitive to low dose irradiation . These measurements are carried out only to confirm that ranges of LED light intensities and reverse bias voltage , that we wish to employ in our characterization , are adequate .

4.2. C -V Plots and Dopant Profile

A typical $1/C^2$ Vs. V plot at room temperature is shown in Fig.4.3. From the slopes in this graph we can obtain the doping concentration and the capacitance values give the distance from the junction at which the slope is measured . We obtain the doping concentration profile of the intrinsic layer this way . The corresponding profile so calculated is shown in Fig.4.4 . Note that at zero bias itself the width of the space charge layer is about 9.3 μm . In conformity with intrinsic character of the active layer the doping concentration is of the order of 10^{12} cm^{-3} . With reverse bias the width can be expanded to 30 - 40 μm Also note that the doping profile does not appear to be a constant . This is typical of commercial samples However this variation in doping concentration is not a serious obstacle to characterization as long as we take it into consideration in the analysis

After irradiation , the depth profile shows some changes in detail though the order of doping concentration remain the same . Fig. 4.5 shows the comparison of doping profile at room temperature These changes are a little suprising since the sample has not been subjected to any high temperature processing .Hence we attribute it to possible changes in experimental artefact such as series resistance . An increase in series resistance decreases the capacitance i.e. the depletion layer appears to be increased . Therefore the doping profile prior to irradiation appears translated to larger distances .

If series resistance is indeed the problem , we would expect it to increase with lowering of temperature . Fig.4.6 shows $1/C^2$ Vs. V curves for the sample after irradiation for several temperatures . Note that the depletion layer width is pushed deeper into the sample for any particular voltage on cooling . If the entire upward shift in $1/C^2$ is attributed to series resistance for each temperature considering that

$$C_m = C_s /(1+ R_s^2\omega^2C_s^2)$$

where C_m is the measured capacitance , C_s is the actual diode capacitance , R_s is the series resistance and ω is the angular frequency corresponding to 1 MHz test signal . Our estimates show that R_s is 1 KΩ at room temperature and varies only to 1 1

KΩ within this temperature range . Hence series resistance does not seem to be playing a major role . The upward shift of $1/C^2$ Vs. V curves are then only due to possible changes in built-in voltage aswell .

In any case the "apparent" doping profiles inferred at low temperatures from C-V data is shown in Fig 4.7 It is observed that for lower temperature the peak and valley structure in the doping profile vanishes and the concentration obtained is roughly uniform It is quite well known that presence of a deep acceptor can in fact result in "apparent" peak and valley features in doping profile [31]. It seems reasonable that at higher temperature this deep trap in the substrate is ionized giving rise to this feature At lower temperatures when carrier capture and emission from this level becomes inactive , this feature vanishes Hence we conclude that this is an artifact due to presence of a deep trap originally in the intrinsic material constituting the active region .

4.3. Absence of Deep Levels Prior to Damage

Thermally stimulated capacitance spectroscopy is a convenient method of an initial survey of deep levels present in the sample . In this method , as explained in detail earlier , the sample is cooled under reverse bias and then at low temperature the traps are filled with a zero bias pulse of required duration .Then the reverse bias capacitance is restored and monitored as a function of temperature for known heating rates . The presence of a thermally activated process in the depletion layer such as release of carriers from the trap is indicated by a step in the capacitance - temperature plot . The position of the step is related to energy of activation and the step height to concentration .

Fig.4.8 shows TSCAP plot for the sample to prior to irradiation . No trace of deep traps are found . It only shows temperature dependence of reverse bias capacitance which is generally caused by changes in carrier concentration with

temperature and variation of Debye length at the edge of the depletion layer . No thermally activated processes are observed .

The other powerful technique to characterize is Deep Level Transient Spectroscopy based on analysis of capacitance transient as explained earlier.

Fig.4.9 shows a typical scan of DLTS which also shows no trace of deep levels. The sensitivity of detection for this run was $2x10^{-3}$ times of background doping which in the present case is of the order of 10^{12} cm^{-3} . This means that in the region of the sample being investigated the trap concentration is less than 10^{9} cm^{-3} . However note that by the above methods we have only investigated distances beyond 9μm from the junction . However high resistive layer typically used in commercial samples are generally uniform and no traps are suspected in the region of the zero - bias depletion width .

4.4. Ion Range And Need For Optical Filling

The range of alpha particles used in this work was determined using TRIM simulations . The range and damage distribution in Si for He^{+} ions of 1.26 MeV energy irradiation is shown respectively in Fig.4.10 and Fig.4.11. Note that the range of the He^{+} and the peak of the damage distribution is at about 4 μm . Hence all the damage is created within the zero - bias depletion layer . Therefore conventional reverse bias DLTS and TSCAP with provision for zero bias filling will not be able to detect the electrically active traps .

At this point it became necessary to augment the existing experimental set-up with facility for optical filling of the traps . This was achieved as pointed out in the last chapter by placing high irradiance infra-red LED in-front of the sample and integrating it to triggering sequence of the existing spectrometer . A current pulse of desired level and time width is pumped into the LED while the sample is zero-biased . This makes the photo-diode forward biased due to generation of both electrons and holes in the depletion layer . The carriers penetrate deep into the depletion layer. We can fill up

traps by this method even if the damage region is well within the depletion layer . The added advantage of this method is that one will obtain information about both majority and minority carrier traps at the same time . This feature is specially of importance when there is need of characterizing prefabricated commercial samples since then one can obtain information about both types of traps at the same time . The only disadvantage is that direct determination of capture cross-section with variable pulse-width filling is not easy since it is to difficult an estimate concentration of carriers reaching the damaged region for capture processes

In the rest of the chapter we concentrate on deep level characterization results with optical filling only

4.5 Optical-DLTS (ODLTS)

As explained in the last section optically filled DLTS (**ODLTS**) is a convenient method for both majority and minority carrier traps .

A typical set of ODLTS curves in the temperature range of 90-300K is shown in Fig.4.12 for different choices of rate window . The peak height is normalized for the dominant peak . The spectra shows three minority carrier peaks labeled E1 , E2 ,E3 and E4 and one majority carrier peaks labeled H1. Except for the peak E4 all other are well resolved . The temperature to the peaks shifts with choice of gates as expected.

From the height of the dominant peak E1 , we estimate the strength of the capacitance transient to be approximately 3pF while the sample capacitance is approximately 2pF . This indicates that $\Delta C/ C$ is approximately 1/ 7 i.e. N_T / N_D ratio is ~ 2/ 7 . That indicates that even as small dose $1\times10^{10}cm^2$ has been able to impart heavy damage . Also note that the damage for the most part is heaviest in the portion where nuclear collisions occur at the end of the range of the ions . Hence the damage is concentrated within a sample volume of approximately 1μm . This further implies that the trap concentration in the region of the damage is at least an order of magnitude

larger then our estimate on the basis of $\Delta C/ C$, which is strictly valid only for uniformly distributed traps in the space change region . Hence the concentration of the traps indicated are in the range of background doping itself (i.e. 10^{12} cm^{-3}) .

Fig.4.13 shows another typical plot for various choices of rate windows ,but this time the extent of filling of the traps has been kept low by reducing the amount of light impinging the sample The height of the peaks is reduced by a factor of 10 and hence non - exponentiality in transients due to large defect concentration is not going to adversely affect our analysis . However note that there is still residual non - exponentiality since the peak height varies dramatically with temperatures at which maximum occurs or the choice of rate window . We defer the discussion of possible sources of non - exponentiality to a later section .

The variation of emission rates with temperature is plotted as a function of 1000/T as in a regular Arrhenius plot to obtained activation energy associated with the peaks . Fig.4.14 shows it four peaks E1 and E2 and from the slope of the least square fitted lines we obtain the activation energy as 0.23 eV and 0 30 eV . Fig. 4.15 shows similar plots for minority and majority carriers peaks whose energies are 0 51 eV and 0.57 eV for peaks E3 and H2 respectively . Before considering detailed discussion of possible origin of these trap levels we briefly consider results of optically filled TSCAP.

4.6.Optically Filled TSCAP

Recall that no evidence of trap levels were found in conventional TSCAP either by zero bias filling or through forward bias filling . Hence we attempted to carry out TSCAP after filling the traps for a low temperature . A typical plot is shown in Fig. 4.16 . The sharp decrease (a step) in the capacitance around 130 K indicates presence of a minority carrier trap in very large concentration corresponding to peak E1 in DLTS . The other steps appear too small to be detected . A differentiation of the TSCAP curve gives peak as shown in Fig. 4.17. This confirms that the major

electrically active defects in the damaged region is due to traps with electrical signature corresponding 0.23 eV trap .

4.7.DLTS Lineshape Analysis

The E1 peak in DLTS curves , corresponding to 0.23 eV energy , showed wide variation in peak height for different rate windows . This is a signature of the corresponding transients being non - exponential . There are several reasons for occurrence of non-exponential transients , chief among them are

- high concentration of defects (comparable to background doping) in which case ΔC is significant fraction of capacitance C .
- presence of series resistance .

spread in energy of activation instead of single discrete energy

In the present case the first two have been eliminated earlier Recall that the series resistance was not so strong so as to affect capacitance measurement significantly . The non-exponential character appeared even when the defect was filled an order of magnitude lower. A surefire method of finding out whether non - exponentiality exists and its origin is to perform lineshape analysis .For this purpose DLTS spectrum is simulated to match the experimental peak position and height . Fig. 4.18. shows a typical spectrum along with a simulated peak for 4.33 msec rate window. Note that the experimental peak is much wider than the simulated lineshape . The broadening observed is nearly symmetric . Since DLTS is a temperature scanning technique it is also important to check that this broadening persists for other temperatures as well We have simulated such spectra for all other rate windows and in each case the experimental curve is wider .The energy and capture cross - section parameters are the same Arrhenius plot as obtained from . Fig. 4.19 shows another comparison with theory and experiment for rate window 31.74 msec . The nature of the broadening in this case suggest that it is composed of many energy levels . It is not clear however whether the energy is continuously broadened or is composed of multiple closely lying energies .

Since DLTS is a temperature scanning technique there is a possibility that the broadened levels are due to change in temperature dependence of sample parameters . It has been argued that the best way to study lineshape is time analyzed transient spectroscopy We go on to do so next .

4.8. Optically Filled TATS Analysis

As described in chapter 3 , TATS spectrum is obtained after DLTS like analysis of isothermal transients recorded over several orders in time . Fig.4 20 shows such a plot for TATS signal against ln(t) which shows both minority and majority carriers peaks . For a particular choice of rate window the maximum corresponding to a particular trap would occur at different times for different temperatures . Hence Arrhenius plots are similar to DLTS can be obtained Since the transients are isothermal , the lineshape of the peaks would have no dependence on temperature Therefore it is most advantageous to rely on lineshape analysis in time domain as in TATS .

Fig.4 21 shows TATS peak corresponding to 0.23 eV peak for two different temperatures . The peak is too broad to be fitted with one exponential transient We have tried to fit the lineshape with two time constants . Though the fit is not as good as one would expect , it certainly shows that multiple peaks are involved .

Similar lineshape fitting is also attempted for the majority carrier peak corresponding to 0.57 eV . Fitting for three different temperatures are shown in Fig.4.22 . The right side of the peaks fit quite well whereas the left side does not fit well due to interference of signal from minority carriers immediately preceding the peak . Fig.4.23 compares Arrhenius plot as obtained from DLTS and TATS . TATS gives an energy of 0.60 eV and as can be seen the time constants are systematically shifted . However in this case DLTS energy seems to be a more reliable guide since judgments about peak position was affected by the presence of nearby peaks . Lineshape analysis also shows that they correspond to exponential transients .

4.9. ORIGIN OF TRAPS OBSERVED

A summary of the parameters of traps observed in the photodiode after 1.26 MeV He^+ irradiation is now tabulated as obtained both DLTS and TATS analysis (given in Table 4.1)

Since the damage is created in the high resistivity region it is not possible to state the type (n or p) of the damaged region with certainty However presence of 0.57 eV peak as majority carrier peak is a direct indicator that the region in which the traps are active is p - type (may be mildly so) This peak have consistently been observed in irradiation induced damage in p - type material The emission signature of 0.57 eV is similar to as reported in B^+ implanted signature Si [32] and Ar^+ induced defects [33] To us it appears that it must be related to heavy damage due to nuclear collisions Hence the DLTS peak H2 seem to be observed implantation induced defects at and $E_v + 0.57$ eV .

The minority carrier peaks are then clearly due to electron traps at E_C - 0.23 eV, E_C - 0.31 eV , and E_C - 0.52 eV peak of these three traps , the one at E_C - 0.23 eV is consistently observed in irradiation induced defects ,and the other two have been reported by some workers . The trap at 0.23 eV is attributed to the first ionization of doubly negative charged divacancy corresponding to $V_2^{--} \rightarrow V_2^{-}$ transition . The fact that this peak is broadened indicates that they occur in a region of damage with disorder and strain so that the energy varies according to the environment . It is likely that it is composed of multiple (possibly two) closely lying energy levels due to disorder. However the most interesting observation is that the transition corresponding to $V_2^{-} \rightarrow V_2^{0}$ which normally gives rise to an electron trap at E_C - 0.42 eV peak is totally absent or not observed in our spectra There has been recently quite some controversy regarding this peak . As discussed earlier in our review it has been found that the ratio of concentration of E_C - 0.23 eV to the one E_C -0.42 eV is dependent on the species used to create the damage. For light ions it has been reported that the observation of E_C - 0.23 is favored [9] . Since in this case alpha particles are used , the predominance of E_C - 0.23 eV over the usual divacancy peak at E_C - 0.42 eV

supports the earlier conjecture of ---------- strongly . It is also probable that this is dependent on the type of the material and is a characteristic of electron deficiency This is a need for further systematic studies in this direction .

The peak corresponding to E_C - 0.30 eV peak has also been observed as an electron trap in ion irradiated material Zafer et al [34] report a similar level in He^{2+} bombarded n -type Si with nearly identical capture cross - section . This level has also been observed by Palmeshofer [8] However a direct correlation with chemical origin has not been possible

The minority carrier at E_C - 0 51 eV has often been associated with extended defects Indusekhar et al [17] report its presence in high energy alpha particle irradiated n - Si where the defects are due to electronic losses alone since the particles escape the sample at the end of the trajectory It is likely that this trap is related to defects created due to electronic losses of energetic particles .

In summary , we have shown that one has to resort to optical pulse filling to characterize deep levels in alpha particle irradiated photodiodes . We have detected four electron traps and a majority carrier hole trap in the irradiated material We show that first ionization of divacancy corresponding to E_C - 0.23 eV is the dominant trap with possible involvement of closely spaced multiple levels associated . The absence of E_C - 0.42 eV trap related to divacancy was striking .

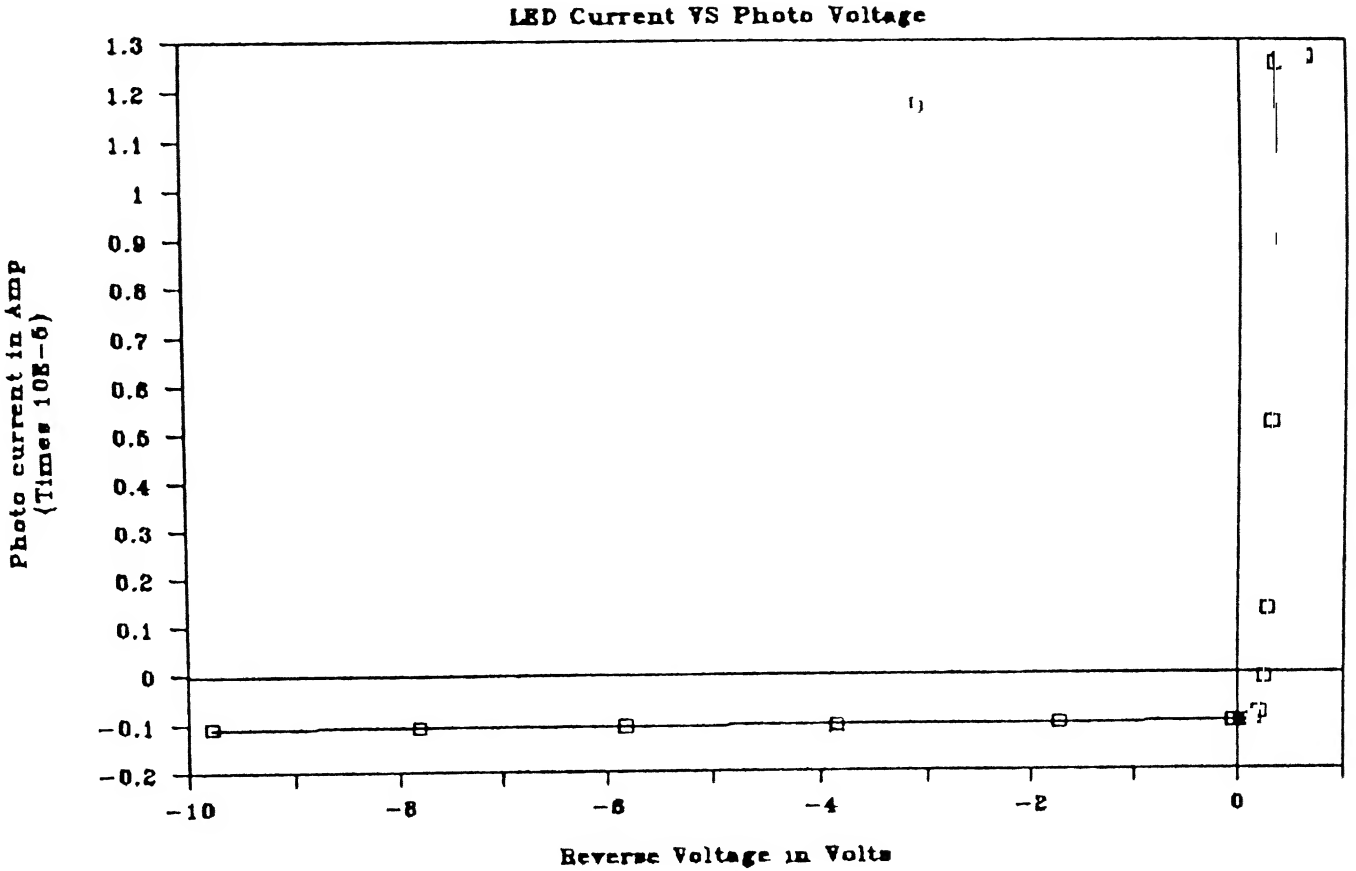

Fig.4.1. Current Vs. Voltage characteristics of the photodiode (for LED current = 20mAmp) .

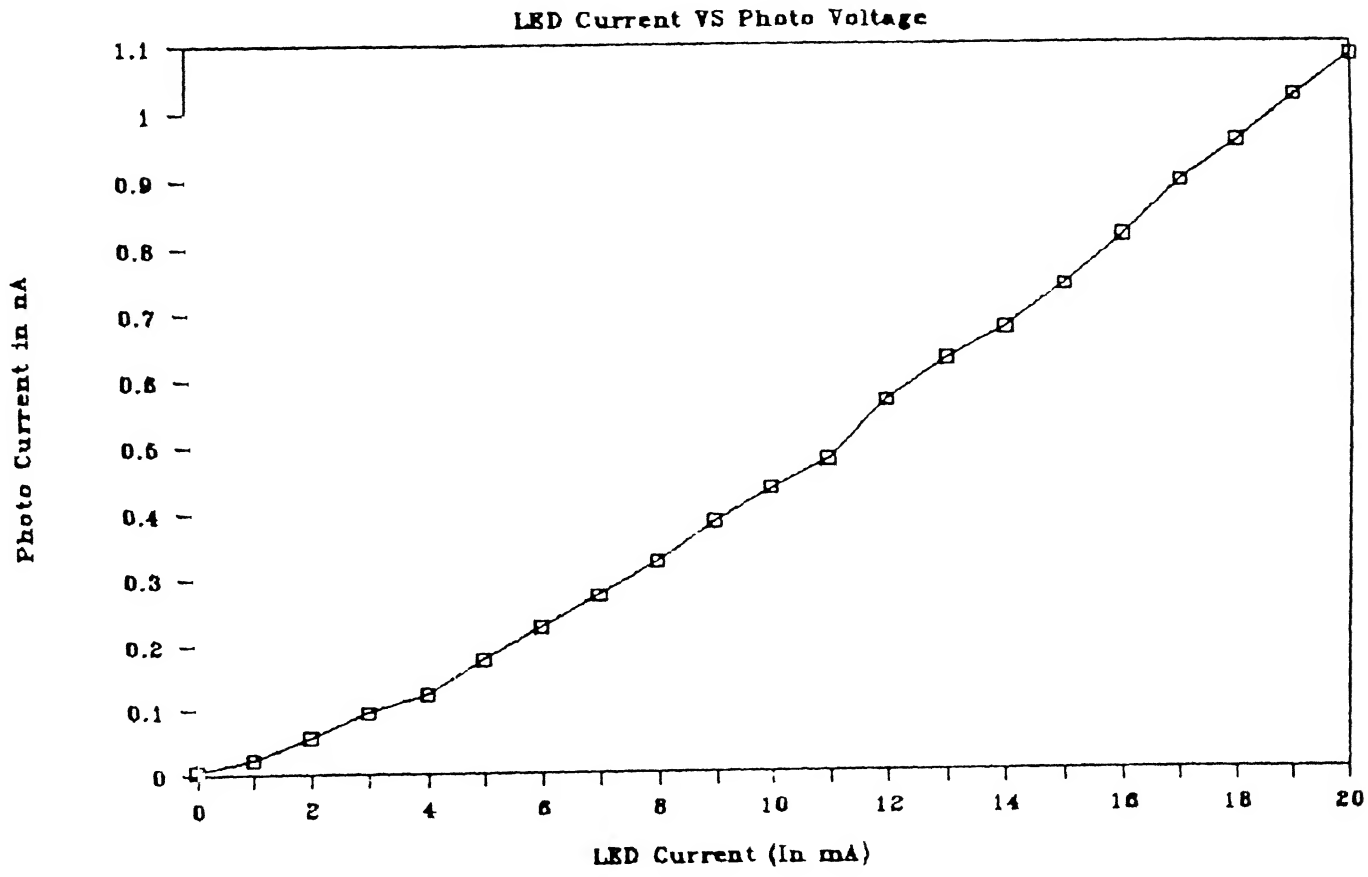

Fig.4.2. Photocurrent Vs. Forward Current in the LED . (Reverse bias = -9V).

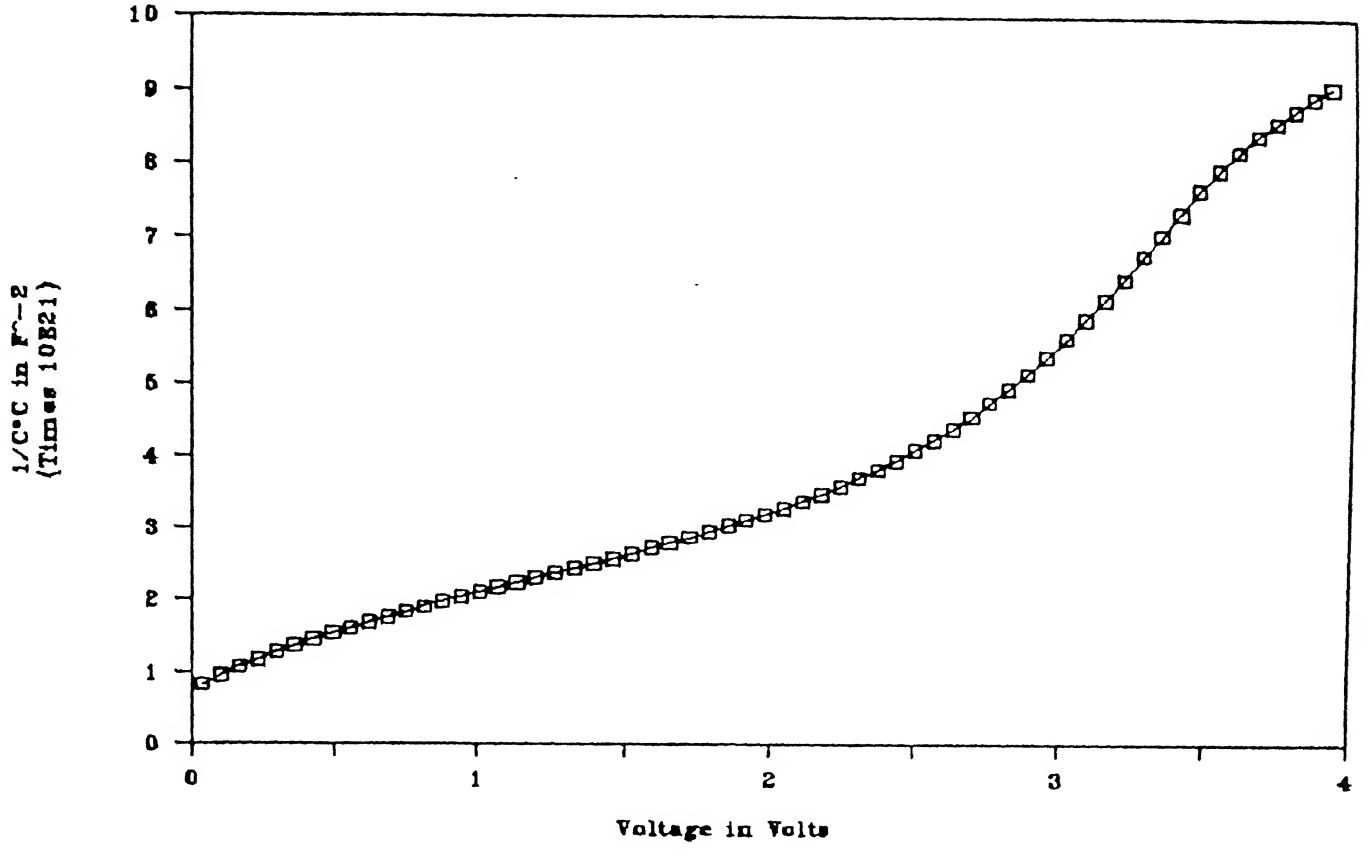

Fig.4.3.Capacitance Vs. Voltage characteristics of the photodiode prior to irradiation (at room temperature T = 296.6 K) .

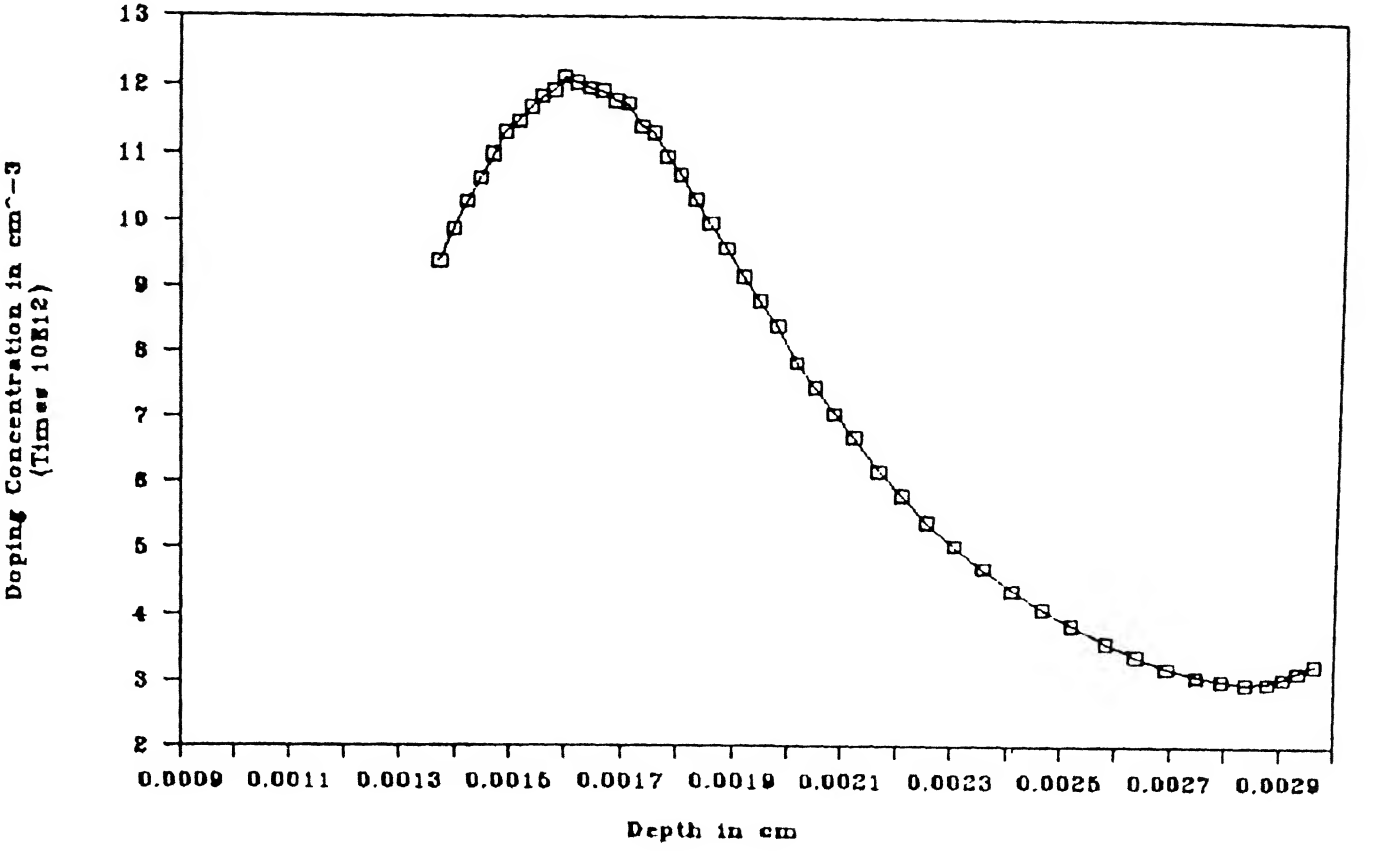

Fig.4.4.Depth profile of photo diode prior to irradiation (at room temperature T = 296.6 K) .

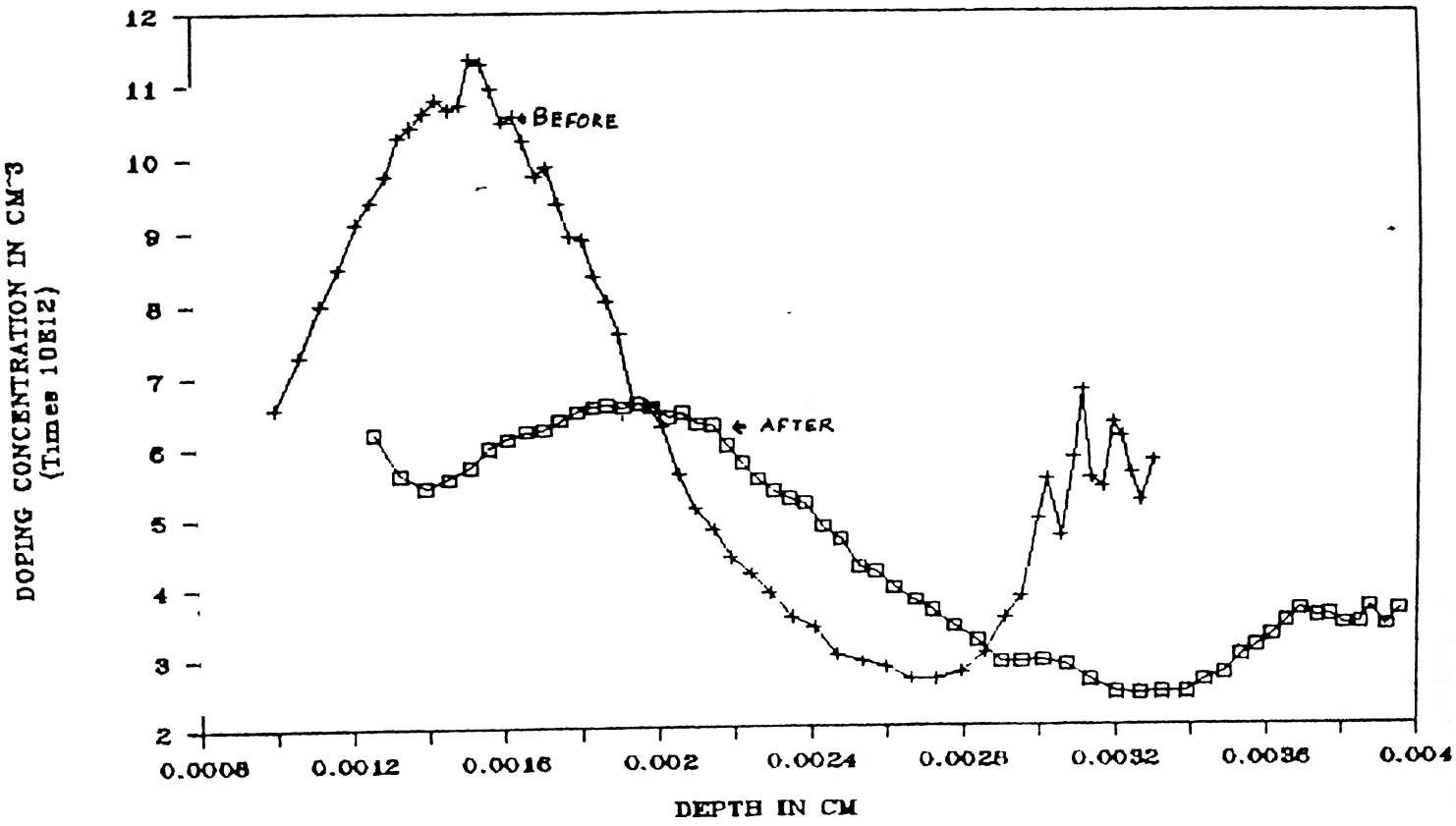

Fig.4.5.Comparision of depth profile of the photodiode before and after irradiation (at room temperature)

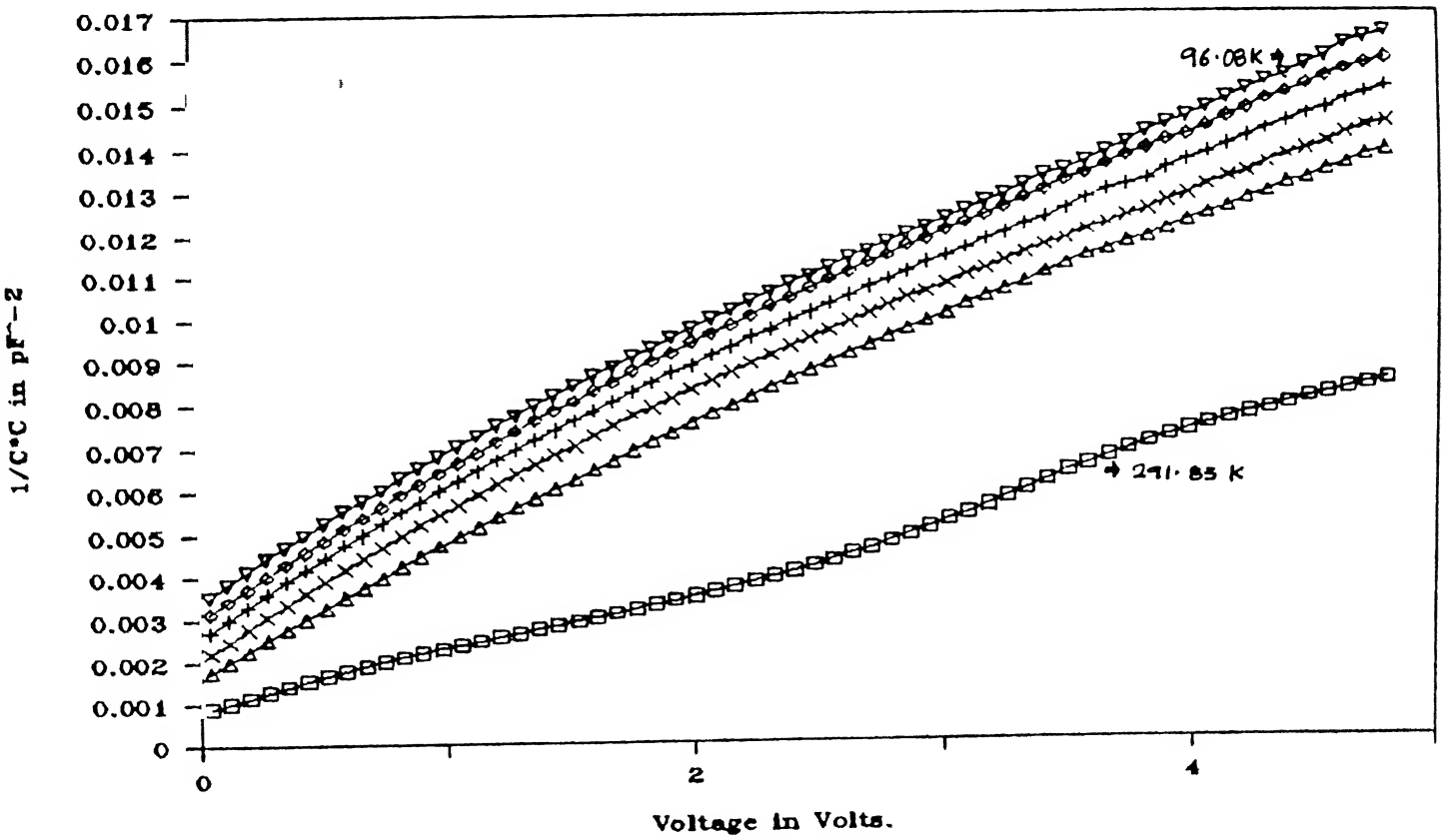

Fig.4.6.Capacitance Vs. Voltage characteristics of the photodiode after damage for several temperatures .

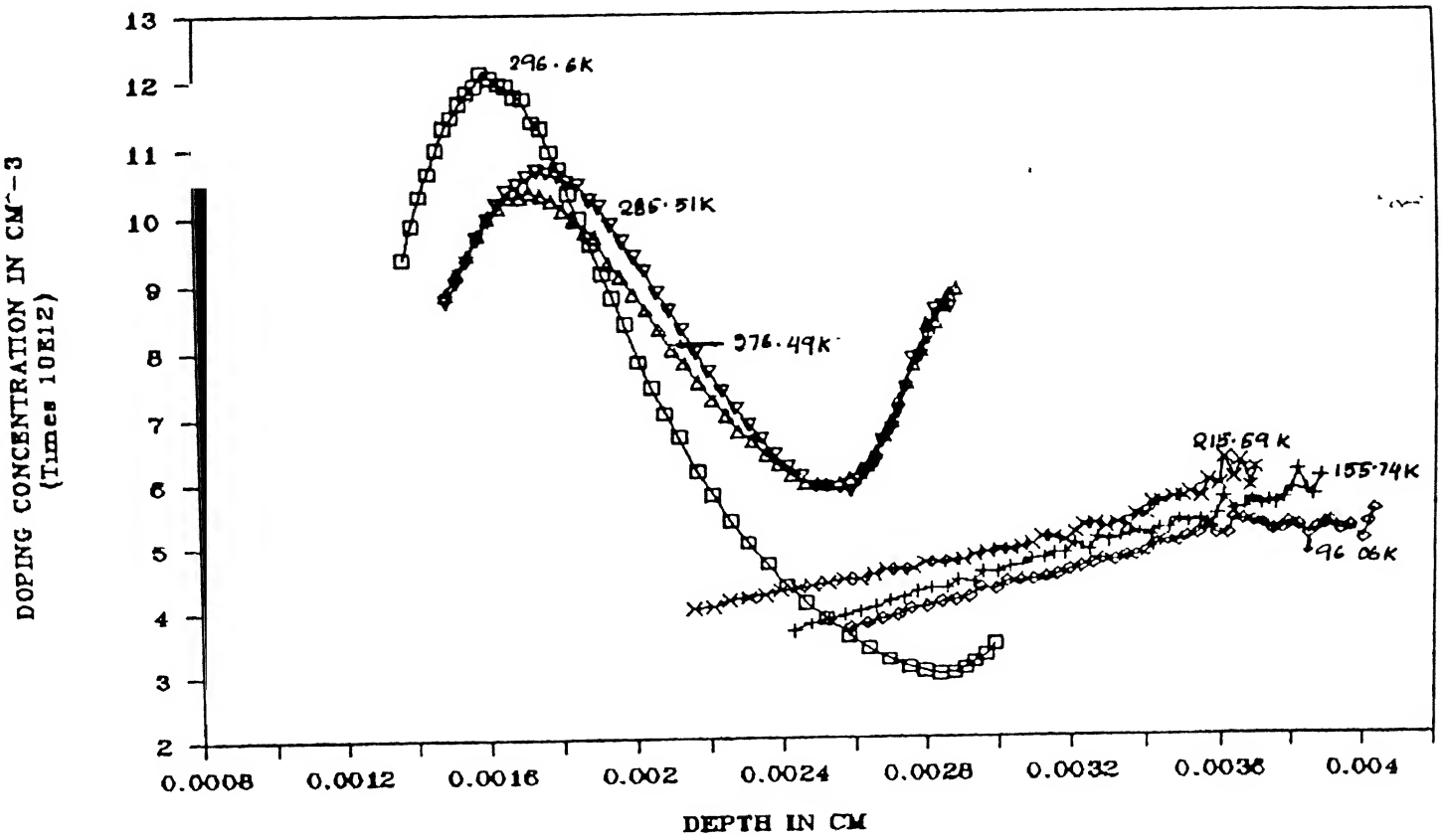

Fig.4.7.Comparision of depth profile of the photodiode after damage for several temperatures .

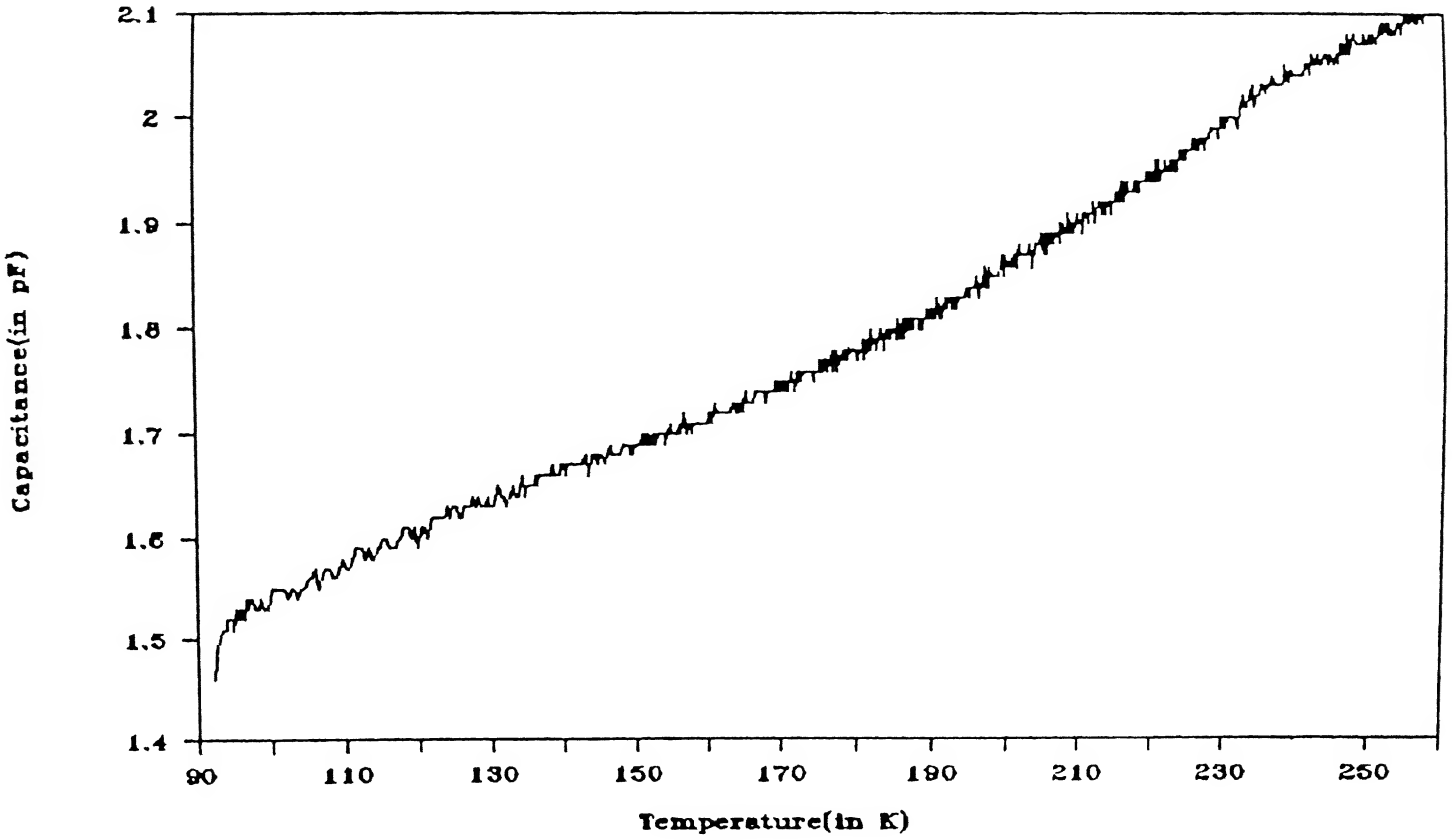

Fig.4.8.TSCAP curve for the photodiode prior to irradiation (for filling time = 30 sec. and heating rate = 1.8 K/min) .

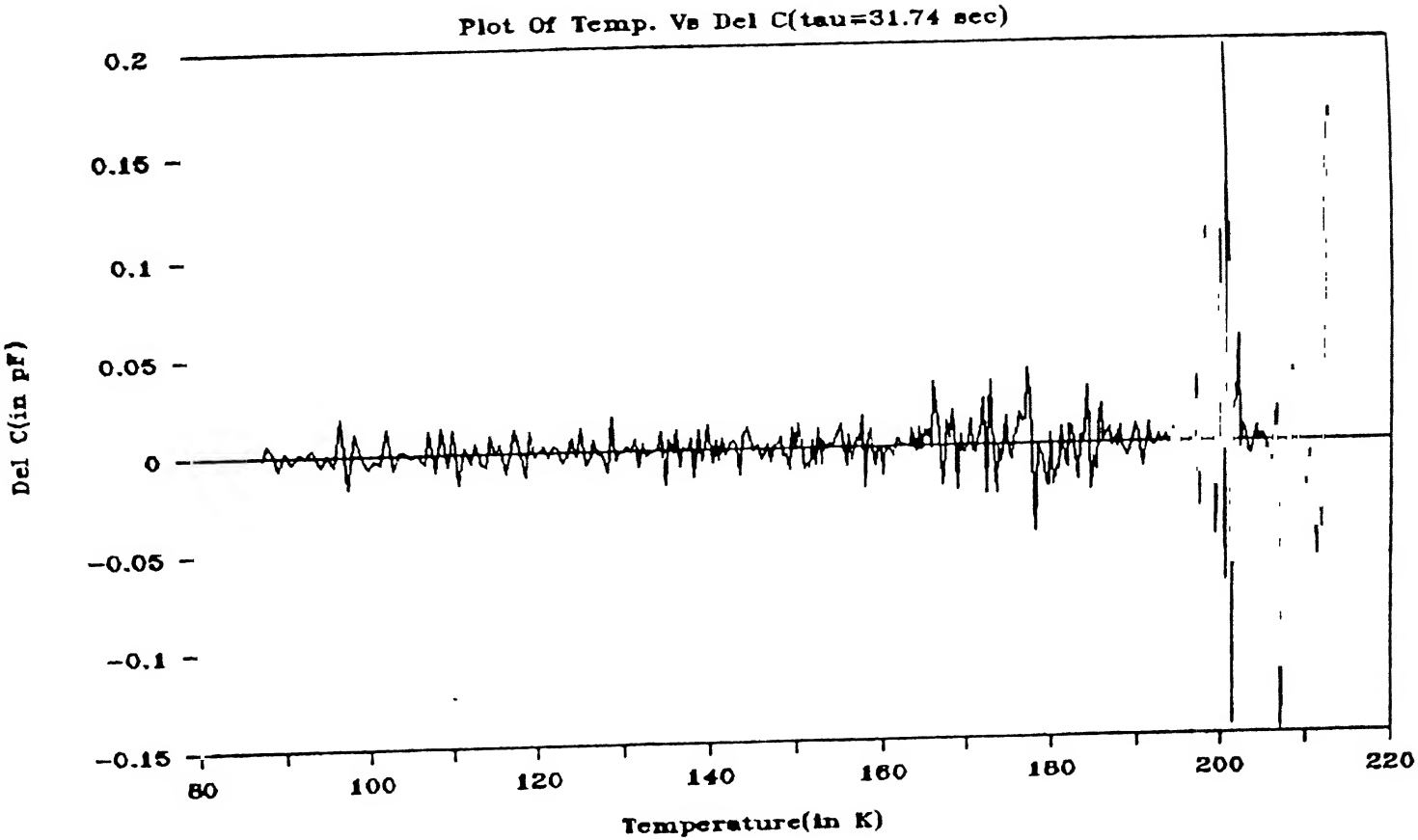

Fig.4.9.DLTS curve for the photodiode prior to irradiation .

TRIM – 1992 (92.12)

ION TYPE = He (4 amu)
ION ENERGY = 1.2 MeV
ION ANGLE = 0 degrees

TARGET LAYERS	Depth	Density
Silicon	200A	19.311
Silicon	6um	2.321

AtomColors=He/He

Ion Completed= 235 (2500)
Backscattered Ions =
Transmitted Ions =

	Range	Straggle
Longitudinal	4.11um	2936A
Lateral Proj.	2410A	3026A
Radial	3673A	1999A
	143.6	

ENERGY LOSS(%)	IONS	RECOILS
Ionization ==>	99.24	0.15
Vacancies ==>	0.01	0.02
Phonons ==>	0.07	0.52

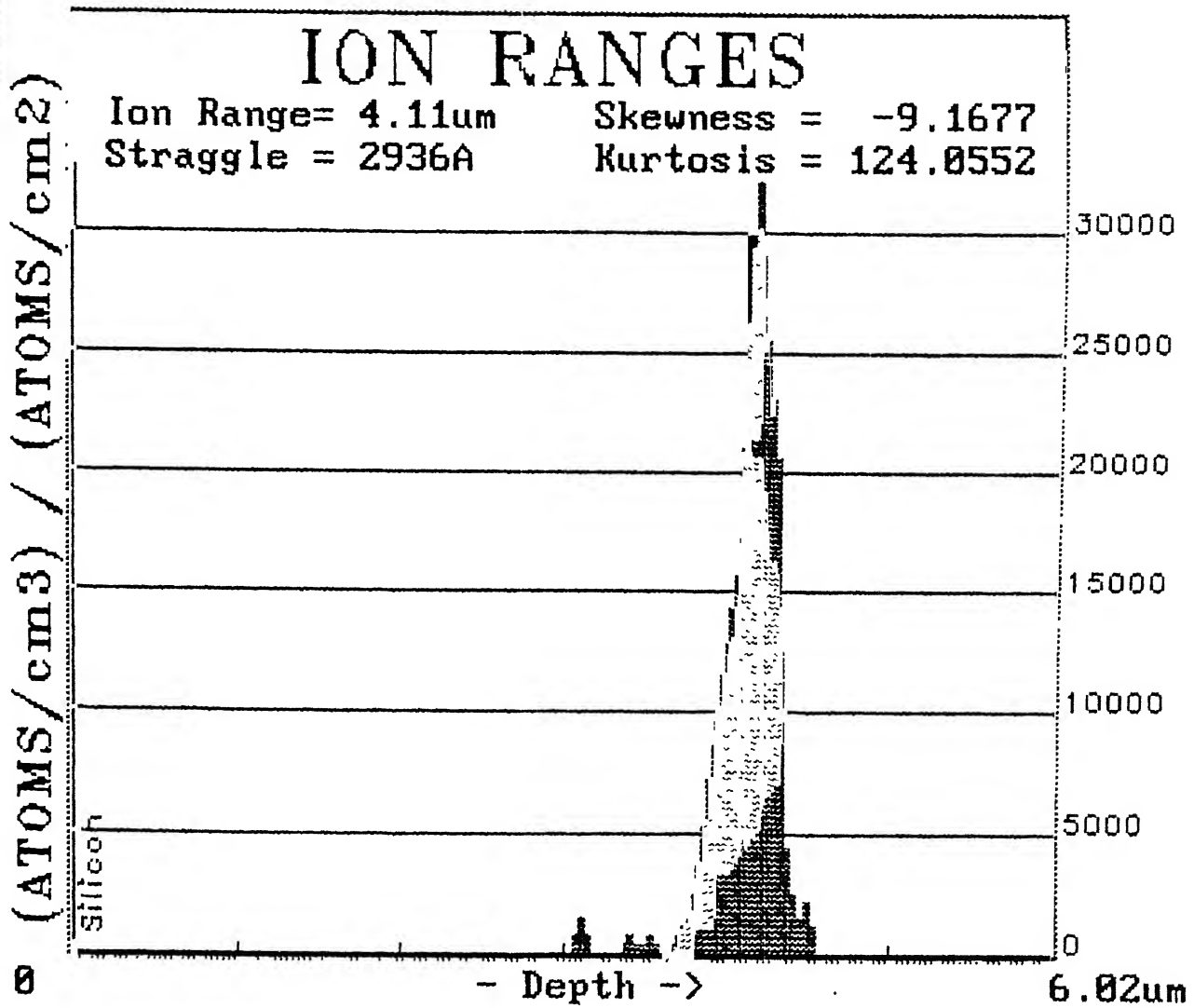

Fig.4.10.He^+ Ions (1.3 MeV ,0°) profile in Silicon .

TRIM - 1992 (92.12)

ION TYPE = He (4 amu)
ION ENERGY = 1.2 MeV
ION ANGLE = 0 degrees

TARGET LAYERS	Depth	Density
Silicon	200A	19.311
Silicon	6um	2.321

AtomColors=He/He

Ion Completed=	235 (2500)	
Backscattered Ions =	0	
Transmitted Ions =	0	
	Range	Straggle
[illegible]	4.11um	2936A
[illegible]	2410A	3026A
[illegible]	3673A	1999A
	143.6	

ENERGY LOSS(%)	IONS	RECOILS
Ionization ==>	99.24	0.15
Vacancies ==>	0.01	0.02
Phonons ==>	0.07	0.52

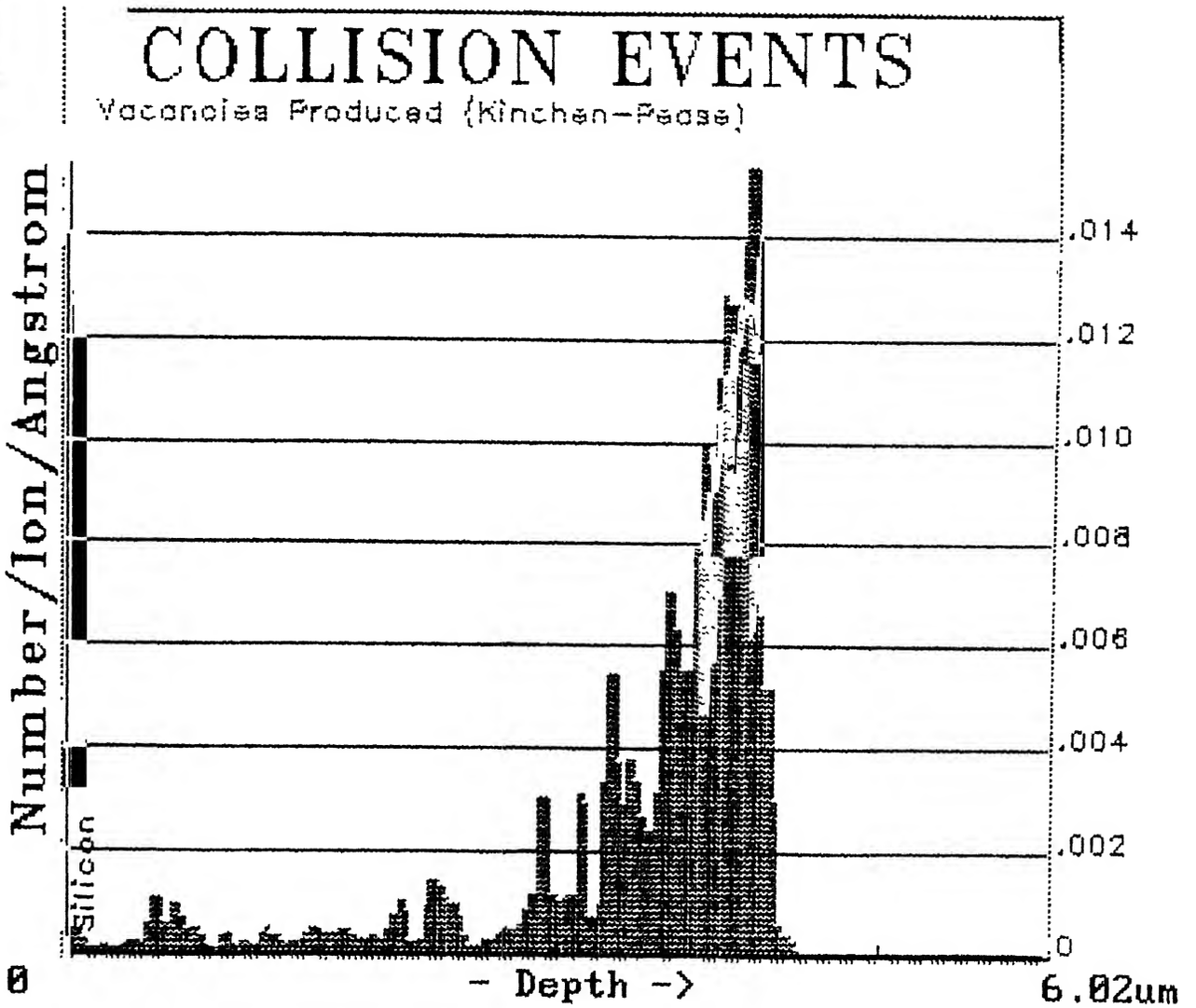

Fig.4.11. Vacancy profile in Silicon induced by He^+ Ions (1.3 MeV,0 °) .

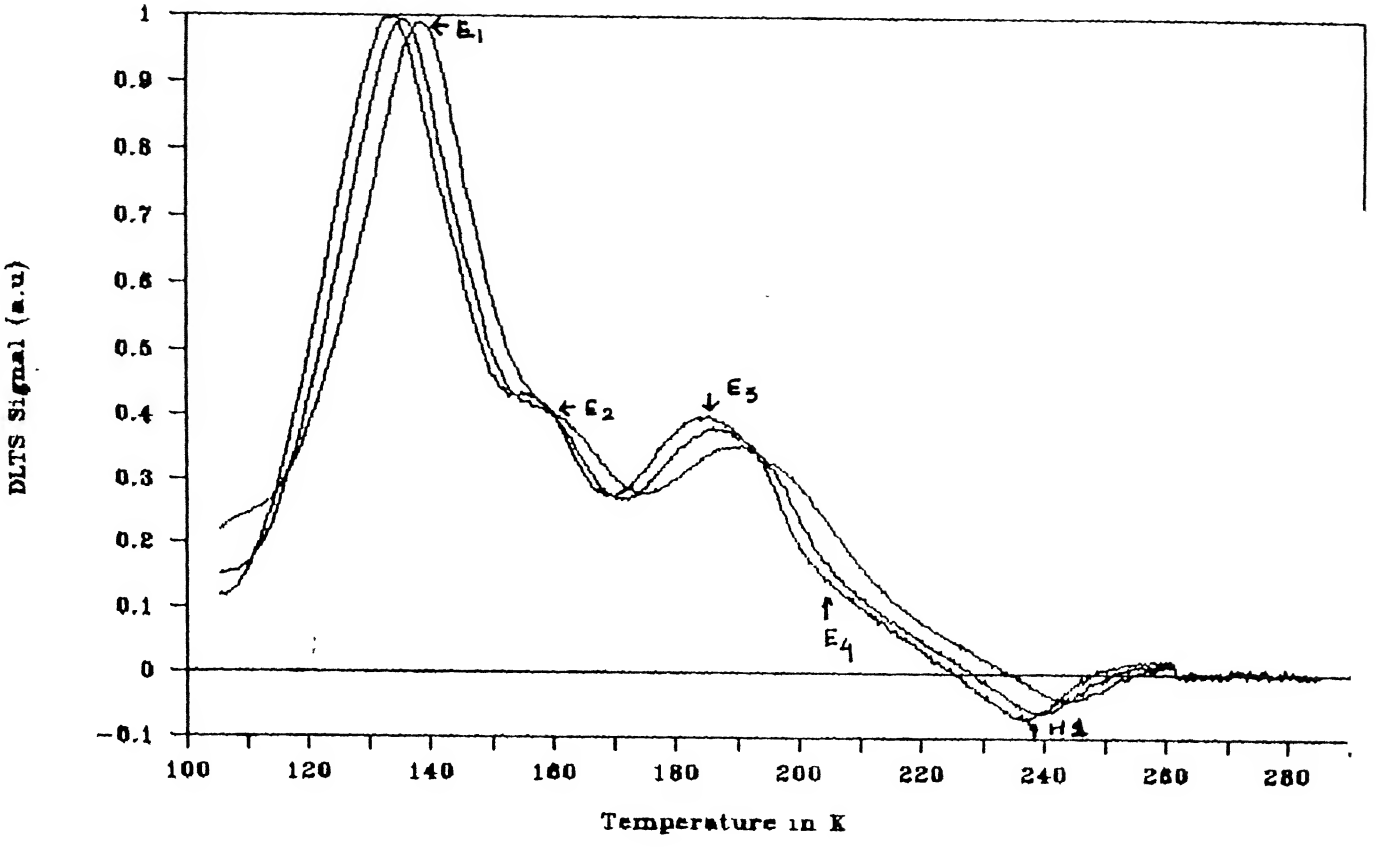

Fig.4.12. DLTS curve for the photodiode after irradiation for three different rate windows.

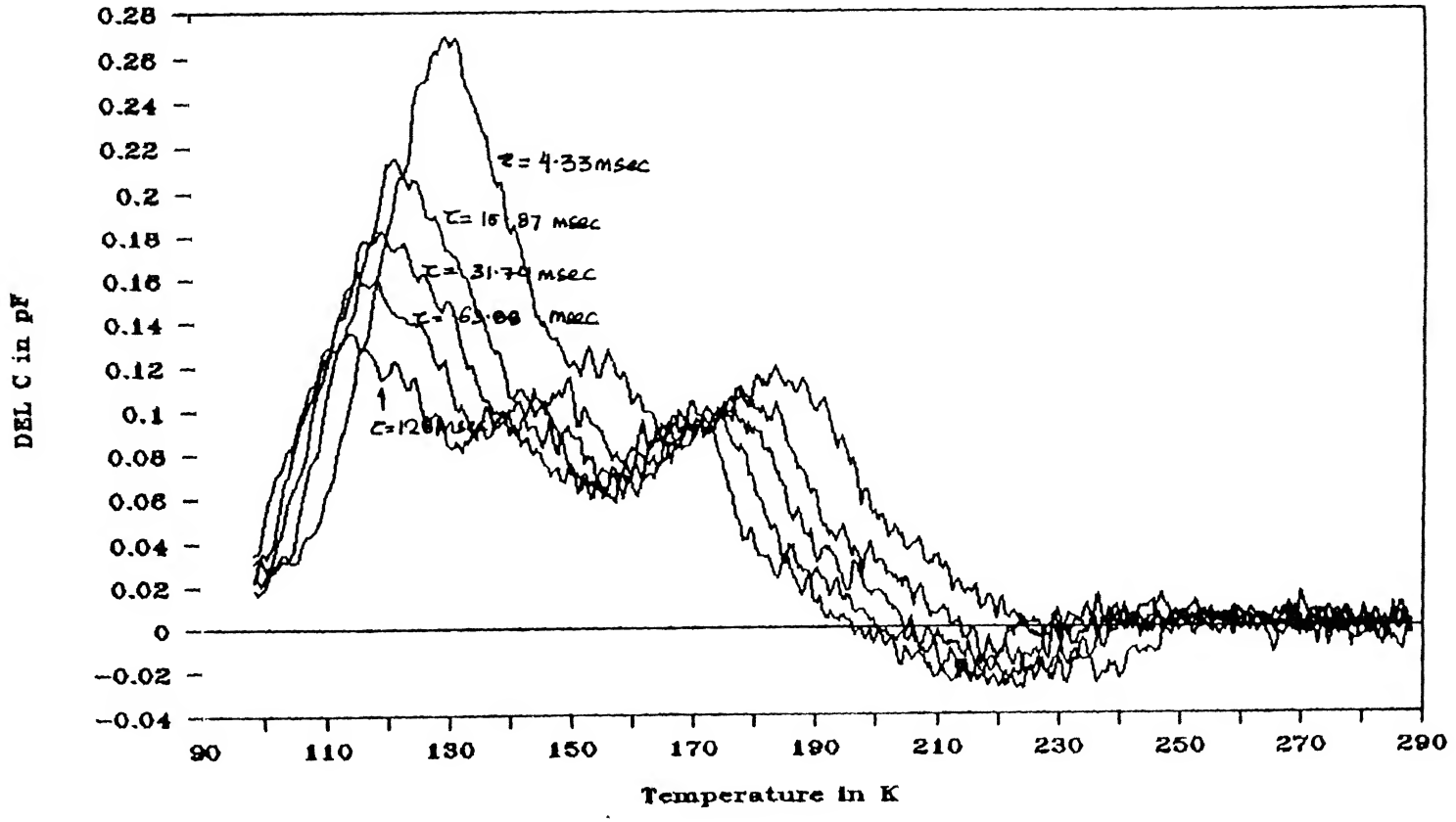

Fig.4.13. DLTS curve for the photodiode for different rate windows .

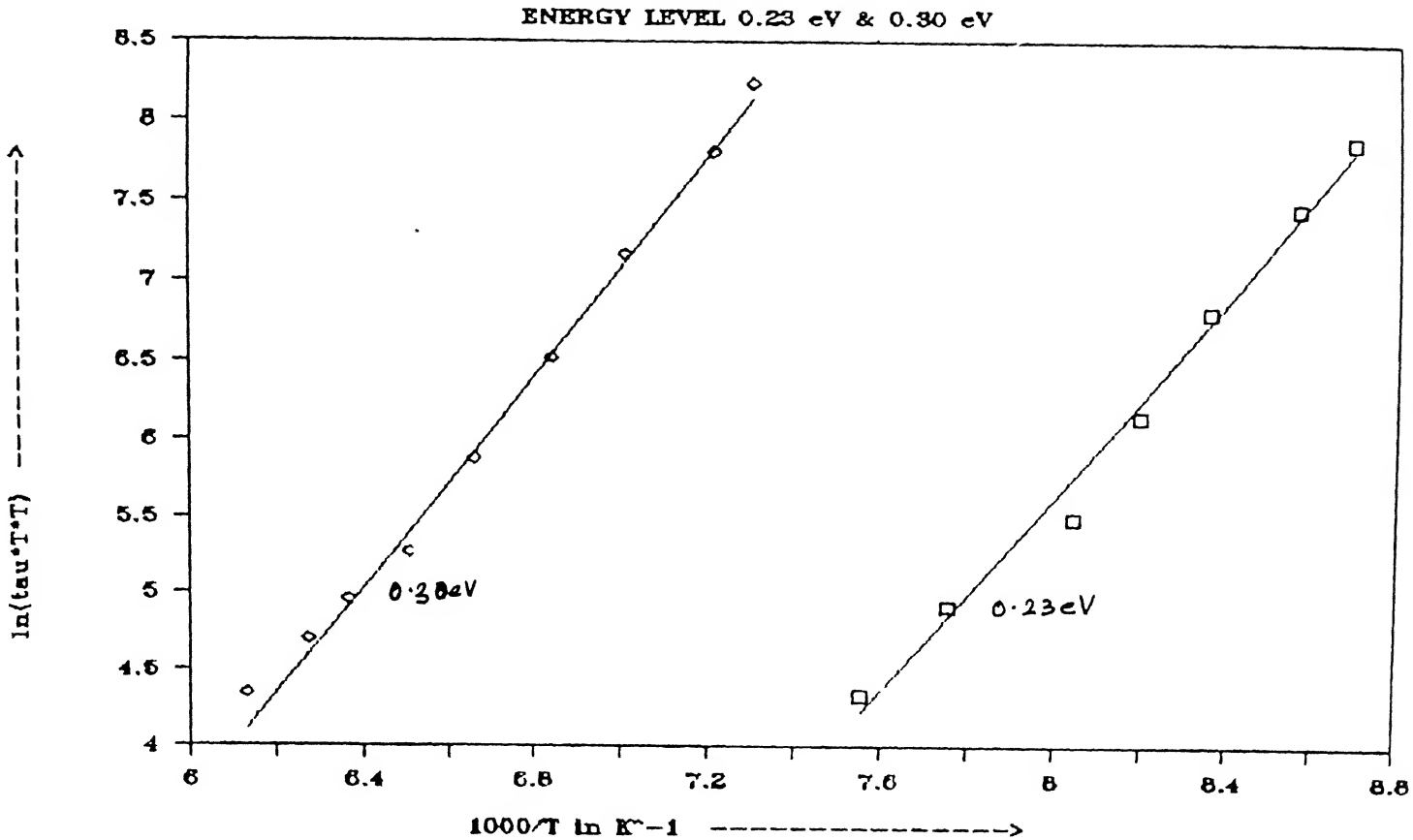
ENERGY LEVEL 0.23 eV & 0.30 eV
ln(tau*T*T) ---------->
8.5
8
7.5
7
6.5
6
5.5
5
4.5
4
0·30eV
0·23eV
6
6.4
6.8
7.2
7.6
8
8.4
8.8
1000/T in K^-1 ---------->
Fig.4.14.Arrhenius plot for two different energy levels (E1 & E2) as obtained from the ODLTS experiment .

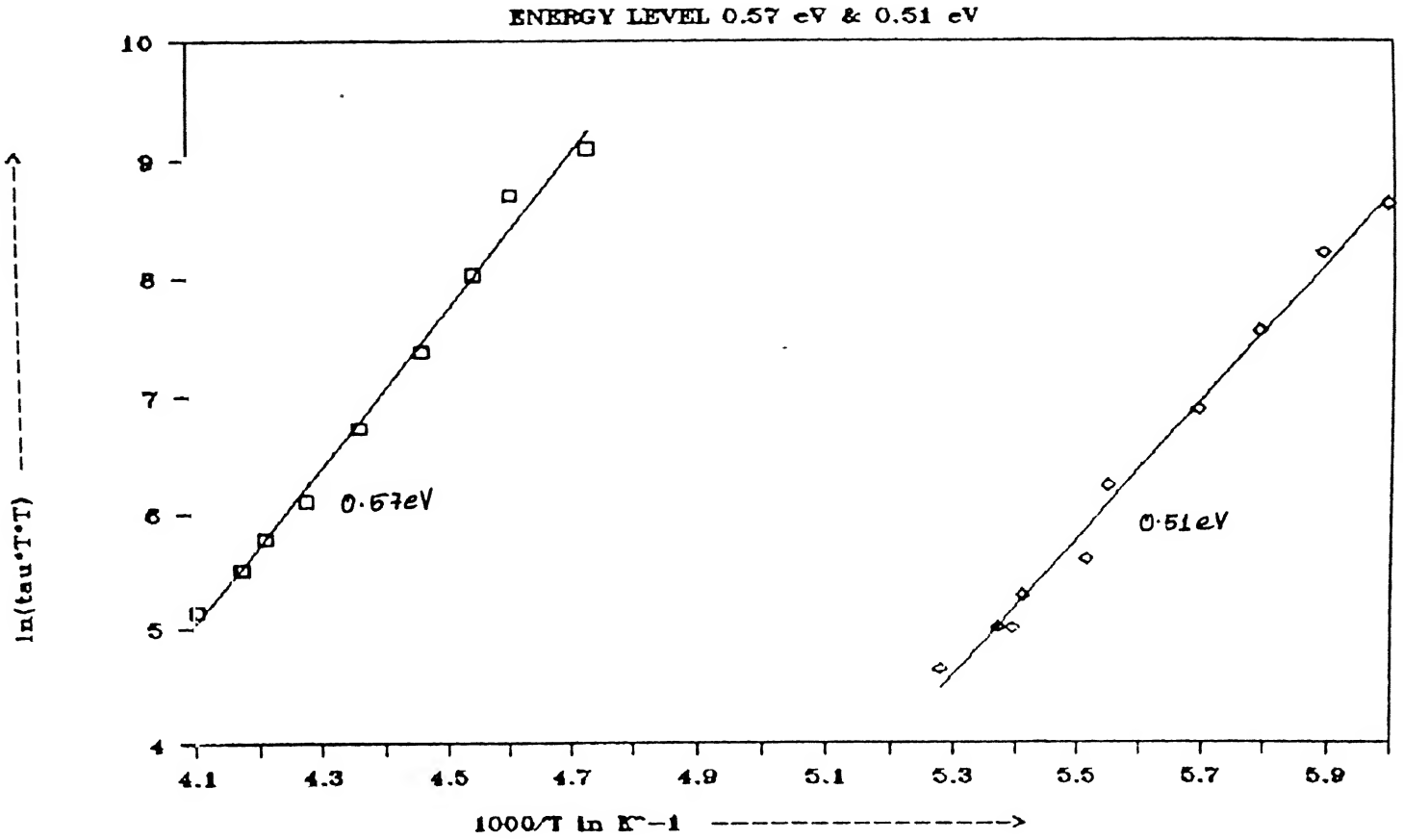

Fig.4.15.Arrhenius plot for two different energy levels (E3 & H1) as obtained from the ODLTS experiment .

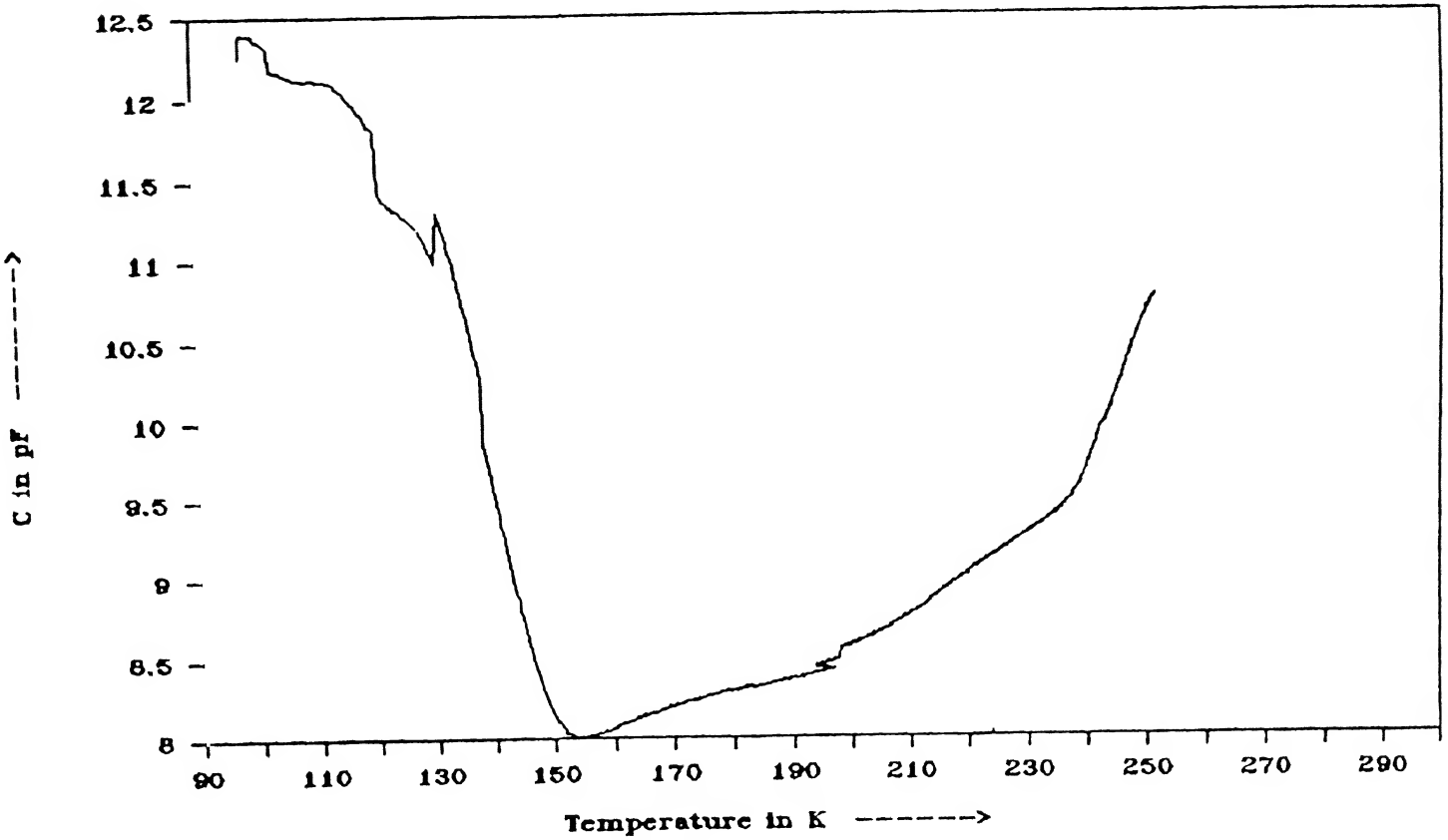

Fig.4.16.TSCAP curve for the photodiode after irradiation (for filling time = 30 sec. and heating rate = 1.8 K/min) .

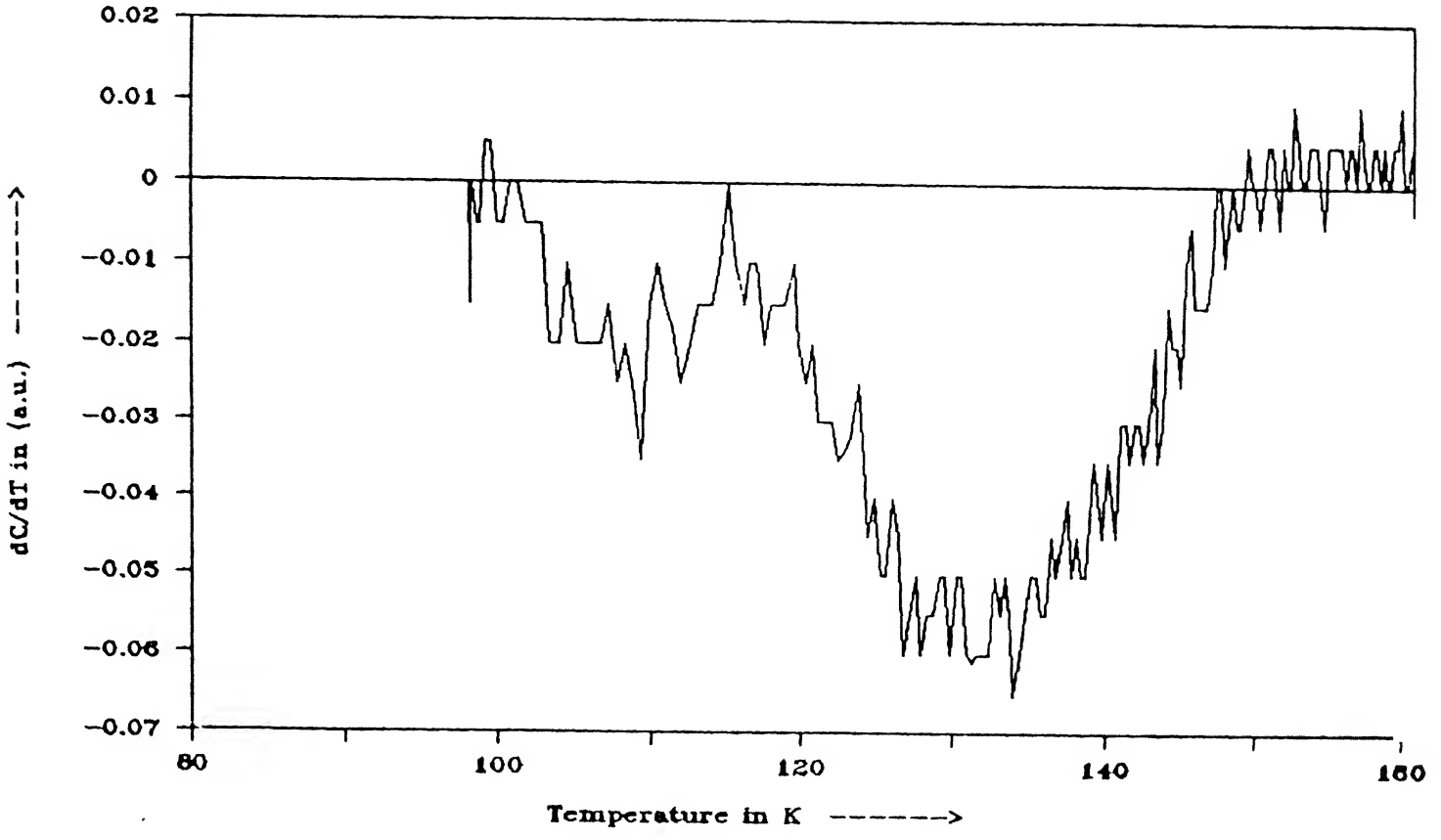

Fig.4.17.Differentiated TSCAP curve for damage photodiode (for filling time = 30 sec and heating rate = 1.8 K/min) .

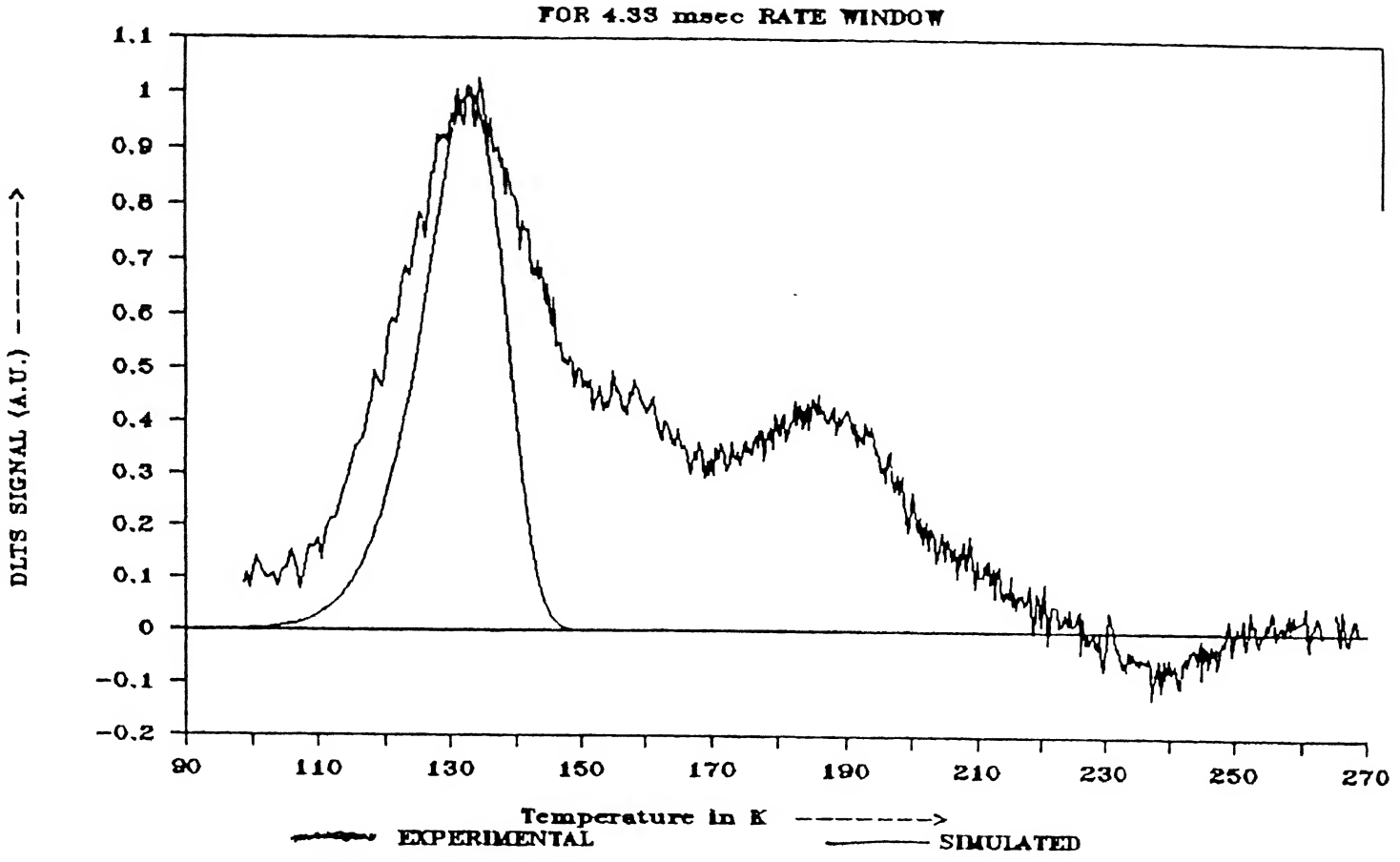

Fig.4.18. Experimental and simulated DLTS curve for E_C - 0.23 eV for 4.33msec rate window.

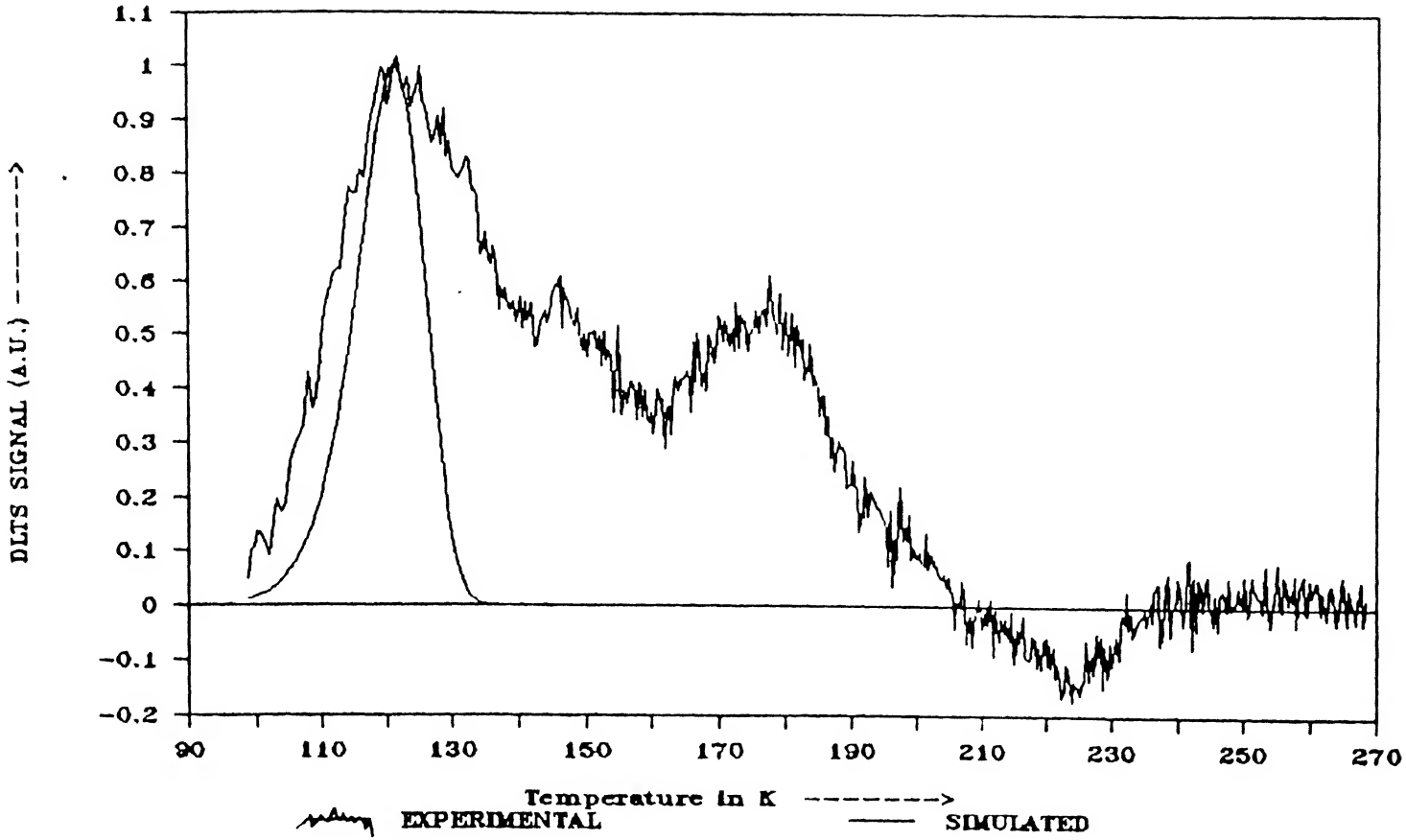

Fig.4.19. Experimental and simulated DLTS curve for E_C - 0.23 eV for 31.17msec rate window .

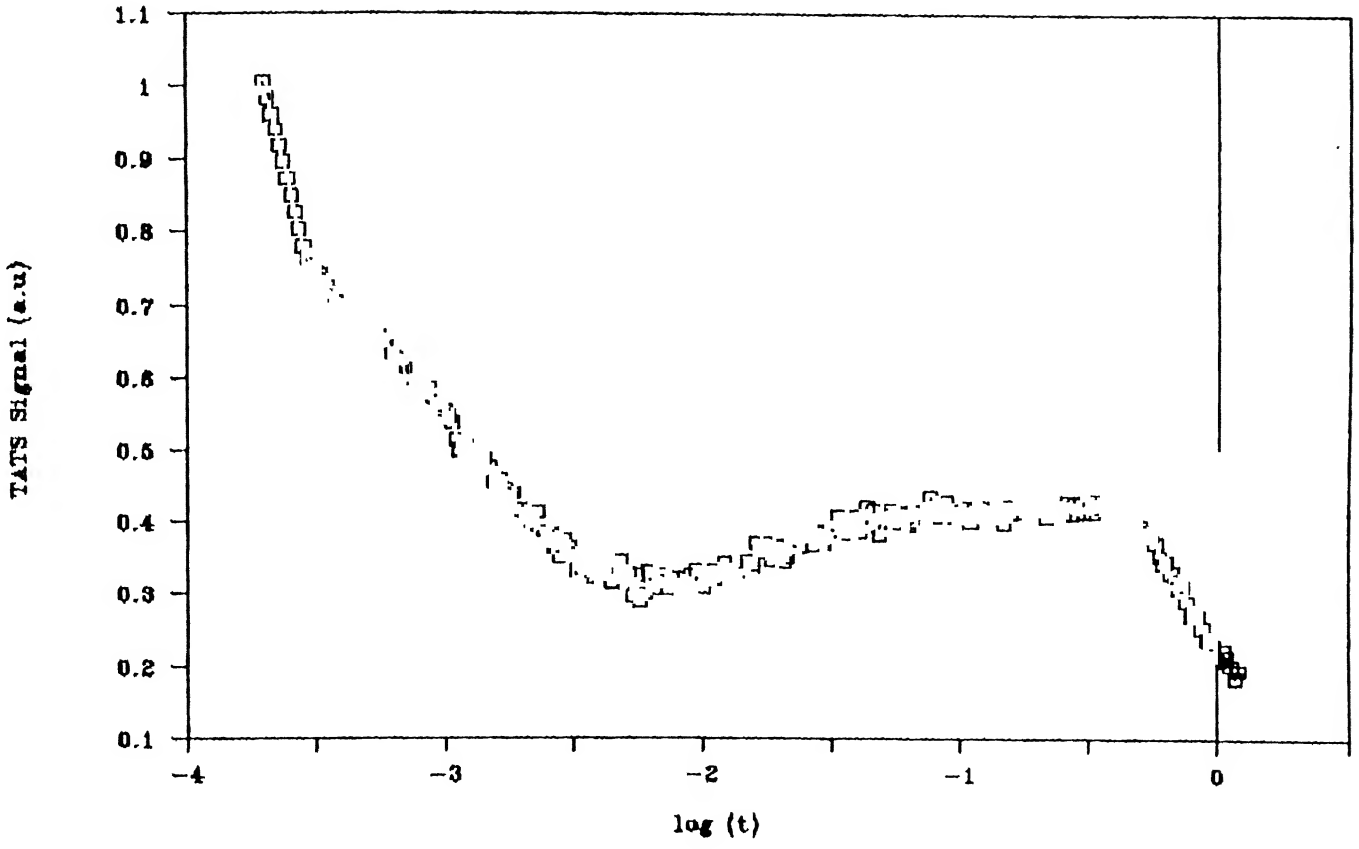

Fig.4.20. TATS spectra of the photodiode after irradiation showing both majority and minority carrier peaks . T= 160·18K

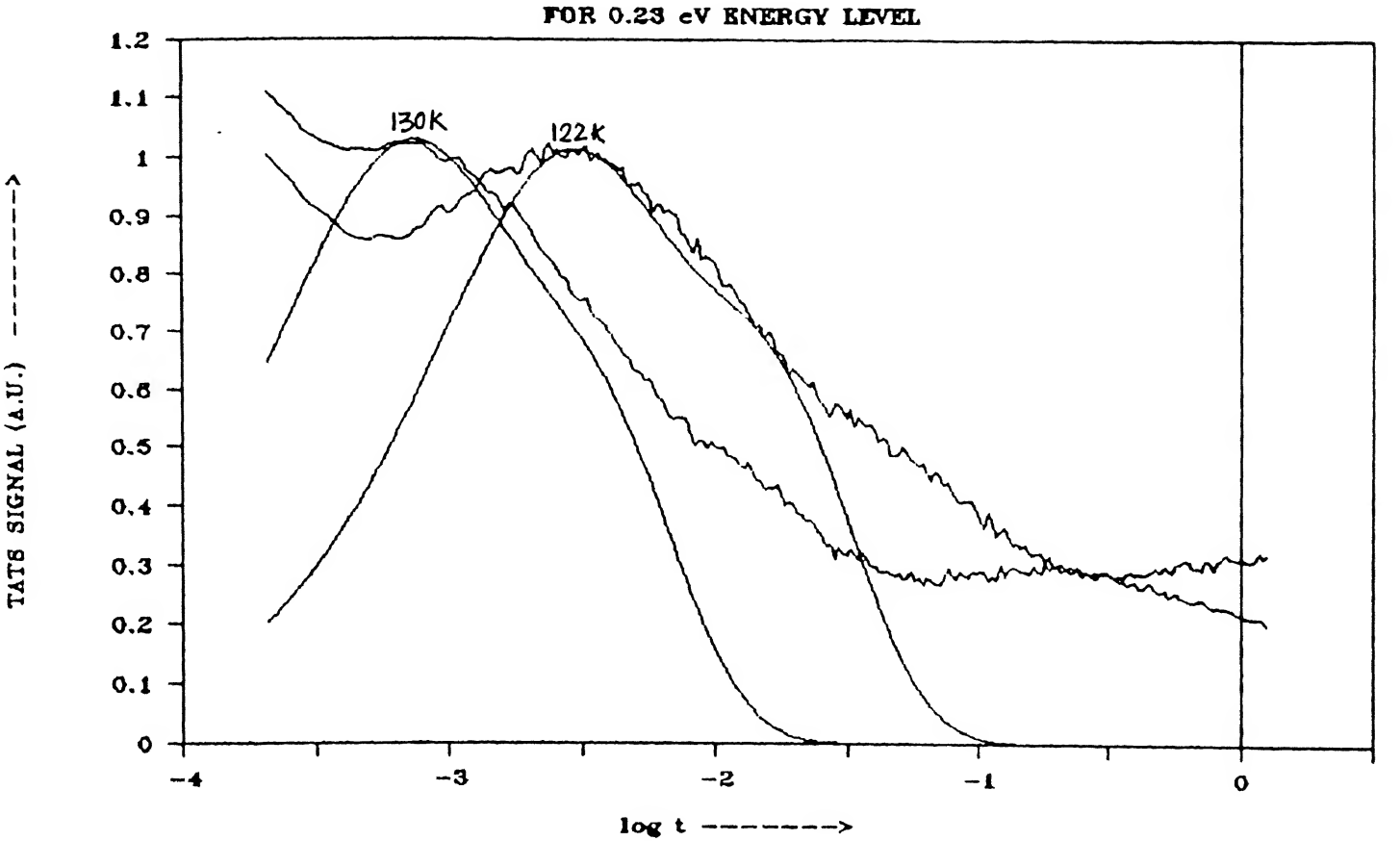

Fig.4.21. TATS spectra corresponding to 0.23 eV peak for two different temperatures with the simulated ones .

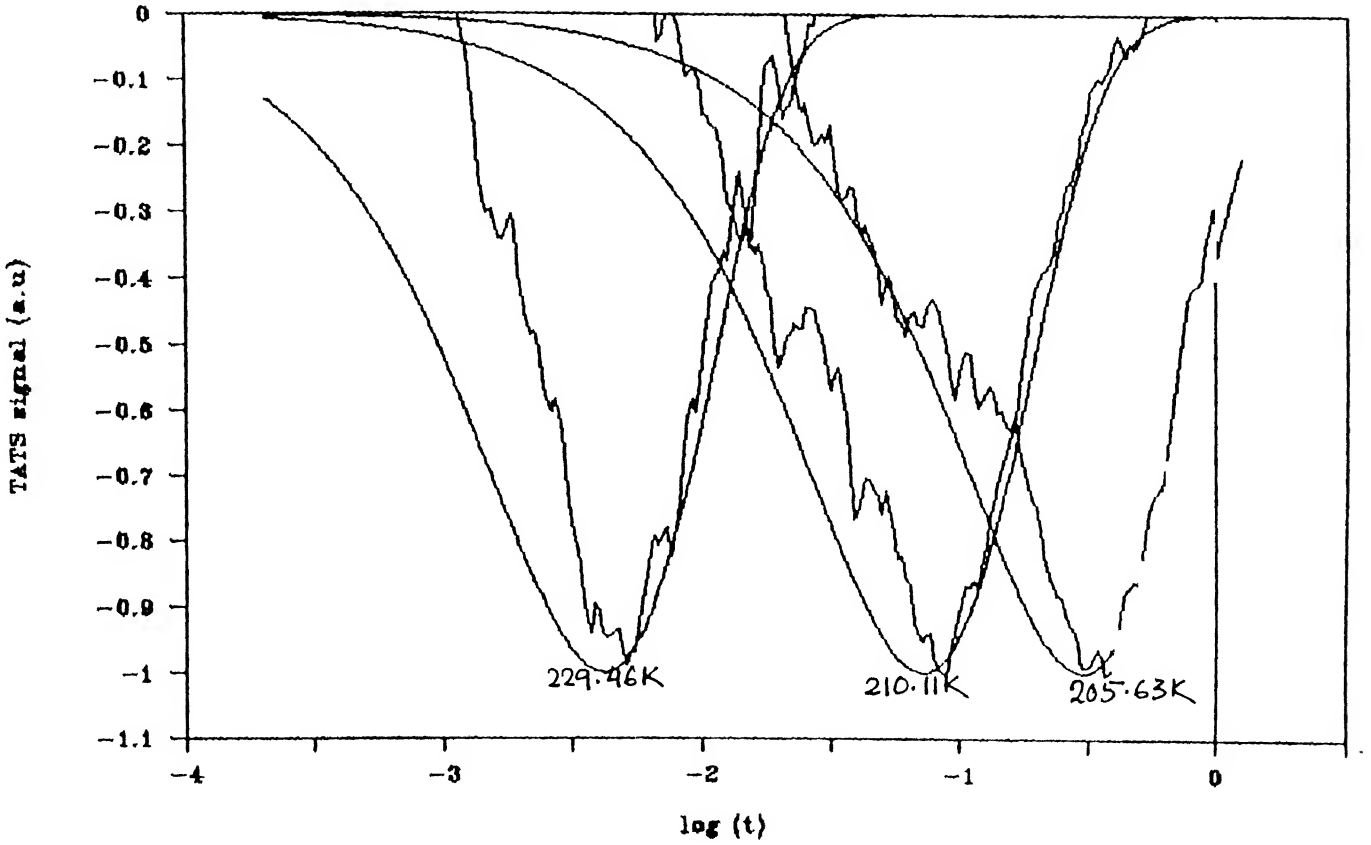

Fig.4.22. TATS spectra corresponding to 0.57 eV for three different temperatures with the simulated ones .

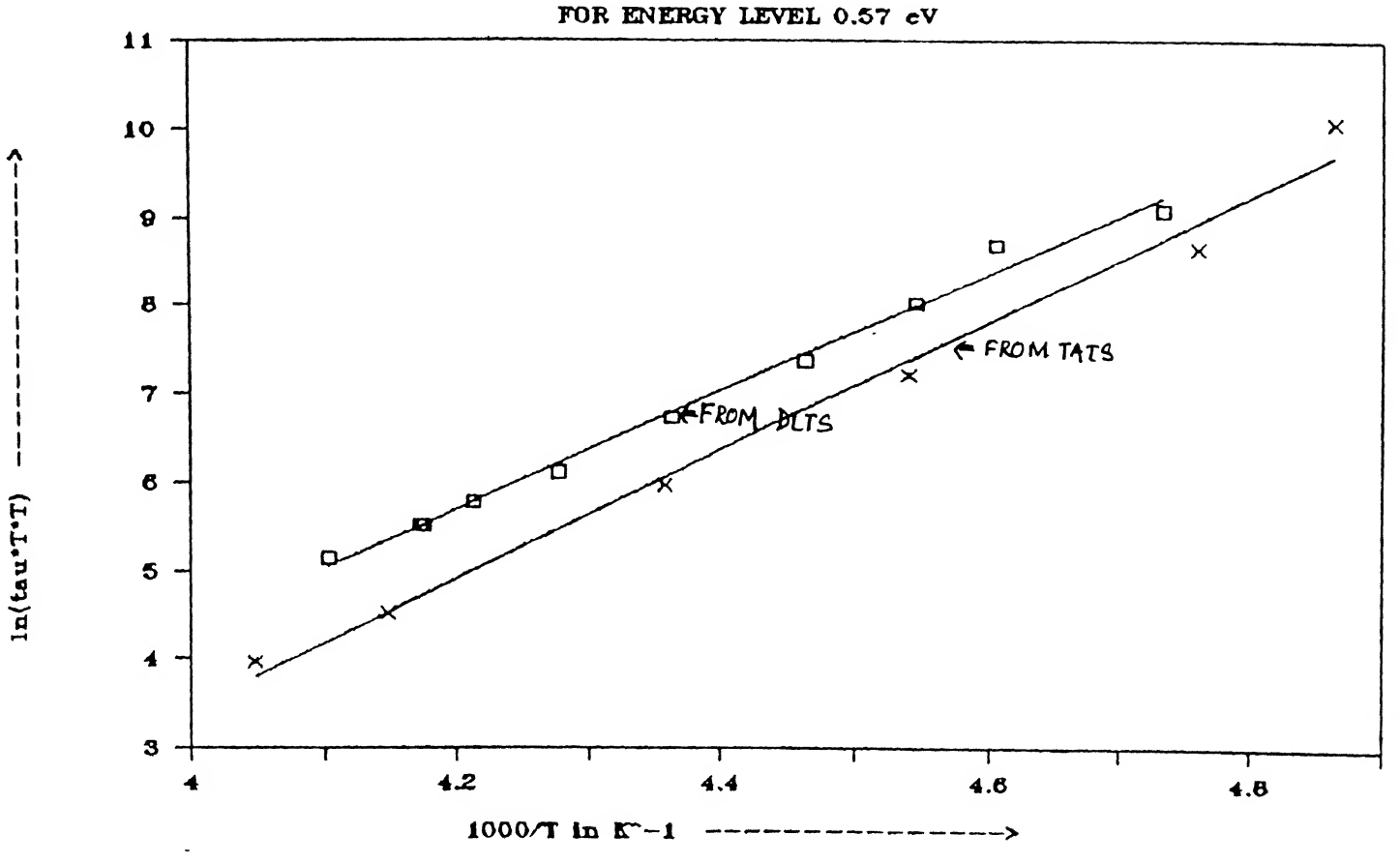

Fig.4.23. Arrhenius plot of the photo diode as obtained from DLTS and TATS measurements .

Table 4.1(a)

Results from DLTS srudy		Results from TATS	
Energy (in eV)	Capture cross-section (in cm^2)	Energy (in eV)	Capture cross-section (in cm^2)
E_C - 0.23	9.05×10^{-15}	0 195	1.87×10^{-15}
E_C - 0.52	4.39×10^{-10}	-	-
E_C - 0 30	2.14×10^{-14}	-	-
E_V+ 0 573	$4\ 30 \times 10^{-12}$	0.60	1.14×10^{-10}

Table 4 1(b)

Parameters for Lineshape Fitting for DLTS			Parameters for Lineshape Fitting for TATS			
Rate Windows (msec)	Energy (eV)	Capture Cross - section (cm^2)	Energy levels (eV)	Tempera ture (K)	Theoritical time constant (msec) τ	
4.33	E_C - 0.23	8.0×10^{-15}	E_C - 0.23	122	3.5	0 7
31.74	E_C - 0.235	$8.0X10^{-15}$	E_C - 0.23	130	17	2.9
			E_V - 0.57	205.63	571.66	
			E_V - 0.57	210.11	133.246	
			E_V - 0.57	229.46	7 41	

Table 4.1(a) Energies and Capture cross - section as obtained from DLTS &TATS .
Table 4.2(b) Fitting parameters for lineshape analysis of DLTS & TATS .

CHAPTER 5

CONCLUSIONS

There is at present a growing importance of using MeV ions as a tool in semiconductor technology . Understanding of damage and related electrically active traps holds the key to eventual success of its use in semiconductor processing technology In this work we choose to study the effect MeV alpha particles in terms of electrically active traps in the active layer of a commercially available Si photodiode . One of the aim is to carry out feasibility of using such samples for MeV implantation studies and issues involved in their characterization

The photodiode is irradiated with 1.26 MeV He^+ ions with a dose of $1x10^{10}$ cm^{-2} at room temperature creating damage upto 4 μm deeper in the sample The sample is characterized using capacitance based techniques such as C-V profiling , deep level transient spectroscopy (DLTS) , thermal stimulated capacitance spectroscopy (TSCAP) and time analyzed transient spectroscopy (TATS) in the temperature range of 90 K - 300 K The existing spectrometer was augmented to be able to carry out optical filling of traps for the purpose of characterization .

The conclusions of the study are as follows:

- Since the zero bias depletion width is very wide due to the intrinsic character of the active layer of a pin photodiode , conventional DLTS and related pulsing techniques are not suitable . Instead optical pulsing to fill the traps was found to be convenient .
- Doping profile showed peak - valley structure at room temperature and it apparently shifted deeper into the sample after irradiation . Any significance variations in doping profile were however not observed at low temperatures indicating that it is most probably due to the activity of a deep trap too fast to be detected by DLTS .
- No active deep traps were found prior to irradiation in the active layer with concentration more than 10^9 cm^{-3} .

- After irradiation three minority carrier peaks and one majority carrier peak was observed in DLTS with concentrations approximately of the same order as background doping Time analyzed transient spectroscopy based on analysis of isothermal transient also show these peaks
- From Arrhenius analysis the activation energies of the traps are found to be 0.23 eV , 0.30 eV and 0.5 1 eV . The majority carrier traps has an activation energy of 0. 57 eV . The 0.23 eV is the dominant peak .
- Lineshape analysis of DLTS signal of 0.23 eV peak shows that it does not correspond to a discrete level in the gap and is probably distributed in energy due to disorder .
- TATS lineshape analysis of the 0.23 eV peak shows that it is more likely to be composed of two closely lying energy levels .
- The majority carrier peak at 0 57 eV is exponential in character , though distorted by the presence of minority carrier peak preceding it .
- The majority carrier trap is attributed to a hole emitting center often found in irradiation induced damage in p- type material . The 0.23 eV is due to the first ionization of divacancy emitting an electron to the conduction band . However corresponding second ionization electron trap at E_C -0.42 eV is not observed probably since its creation is suppressed for damage induced by light particles The other peaks are tentative associated with E_C - 0.30 eV and E_C - 0.51 eV traps reported in the literature of ion irradiation induced defects .

In summary , optical filling pulse in conjunction with DLTS and TATS was necessary to characterize both electron and hole traps in MeV alpha particle induced traps in a photodiode . It is found that , though use of photodiode is convenient for MeV ion studies as far as physics of defects is concerned , certain quantitative aspects such as direct determination of capture cross section , deep level trap profiles etc. , are difficult . The disadvantages are principally due to the large space charge layer that gets created in the active layer . The effects of introducing traps in the active layer and their role in determining device characteristics can be easily studied using the methods developed . Future studies in this direction would be fruitful , specifically in controlling life time . The commercially available photodiodes do provide an extremely convenient

structure for characterization studies of deep defects induced by MeV ions inspite of the disadvantages encountered during the course of this work .

BIBLIOGRAPHY

[1] Radiation effect in semiconductors (Inst. Phys. Cond . Series)

[2] E. Chason , S.T. Picraux , J. M. Poate, J.O. Borland , M. I. Current , T.D .de le Rubia, D.J. Eaglesham, O.W. Holland , M.E. Law ,C.W. Magee , J.W. Mayer, and A.F. Tasch , J . Appl Phys . , **81**, 6513 (1997)

[3] Troxell J.R . , Solid State Electronics ,**126**, 539(1983)

[4] P.K .Giri ,Phd Thesis ,IIT Kanpur , India(1997)

[5] G.D.Watkins and J.W.Corbett ,Phys. Rev.,**138**,A, 543(1965)

[6] Cheng L.J. et al , Phys. Rev., **152** ,761(1966)

[7] L.C. Kimerling ,IEEE Trans. on Nucl .Sci ,**23**, no.- 6 (1976)

[8] L.Palmeshofer , J.Resinger , J.Appl. Phys. , 72(6),2167(1992)

[9] B.G.Svensson , B.Mohadjerv , A.Hallen , J.H.Svensson , and J.W.Corbett ,Phys. Rev.**B 43**,2292 (1991)

[10] B.G.Svensson and M.Willander , J.Appl . Phys. ,**62**,2758 (1987)

[11] J.L.Benton , S.Libertino , P. Kringhoj , D.J.Eaglesham , J.M.Poate , and S. Coffa , J.Appl.Phys. ,**82**,120(1997)

[12] K.L.Wang , Appl. Phys. Lett., **36**,48 (1980)

[13] G.D.Watkins and J.W.Corbett , Appl. Phys. Lett. ,7,314 (1961)

[14] A.Hallen ,P.A.Ingemarsson , P. Hakansson , G. Possnert , B.U.R. Sundqvist , Nucl. Instrum. Methods B **36** , 345 (1989).

[15] L. Palmetshofer and J. Reisinger , Appl.Phys.Lett. **59(27)**,3583 (1991) .

[16] Hallen et al., J.Appl.Phys. **70**, 3025 (1991) .

[17] Indusekhar H , Phys. Stabs . sol. , **93 (a)** , 645 (1986) .

[18] Berman L.S. , Soviet Phys. Semicond , **152** , 665 (1981).

[19] Lang D.V. , J. Appl.Phys. , **45,No7**,(1974)

[20] L.C.Kimerling,Radiation damage in semiconductors -1976,Inst.Phys.Conf.Ser.**31** 221 (1977)

[21] G.D.Watkins and J.W.Corbett,Phys.Rev.,**121**,1001(1961)

[22] L.C.Kimerling et al, Solid St. Comm.,**16**,171 (1975).

[23] Ramakrishna , M.Tech Thesis ; IIT Kanpur , India (1997)

[24] M.Mamor, F.D.Auret, S.A.Goodman, W.E.Meyer, Mat.Res.Soc.Symp.Proc., **510**,449. 1996

[25] D.K.Shroder,Semiconductor Material And Device Characterization, (John Wiley & Sons , Singapur , 1990), Ch7

[26] A.G.Milnes, Deep Impurities In Semiconductor

[27] C T.Sah,L.Forbes,L.L.Rosiser And A.I.Taschjk, Solid State Electronics ,**13**,759 (1970)

[28] Sandeep Agarwal , Y N.Mohapatra And V.A.Singh, J.Appl.Phys.,**77**,3155(1995)

[29] Banerjee N,Ph.D. Thesis ; IIT Kanpur , India (1993)

[30] Chaudhuri ,Ph.D. Thesis ; IIT K , India

[31] L.C.Kimerling,J.Appl.Phys ,**45**, 1839(1974)

[32] H.Sayama,A.Kinomura,Y Yuba And M.Takai, Nucl Instum . Methods Phys . Res **B 80/81** , 787 (1993)

[33] P.K.Giri , S.Dhar , V.N.Kulkarni , Y.N.Mohapatra , NIMB **B 111**,285(1996)

[34] M.Asghar, M. Zafer Iqbal , and N.Zafar , J.Appl . Phys. ,**73**,3698(1993)

Date Slip

This book is to be returned on the date last stamped.

.....	.....
.....	.....
.....	.....
.....	.....
.....	.....
.....	.....
.....	.....
.....	.....
.....	.....
.....	.....
.....	.....
.....	.....